National Library of Canada
Canadian Theses Service
Ottawa, Canada
K1A 0N4

Bibliothèque nationale du Canada
Services des thèses canadiennes

# CANADIAN THESES

# THÈSES CANADIENNES

## NOTICE

The quality of this microfiche is heavily dependent upon the quality of the original thesis submitted for microfilming. Every effort has been made to ensure the highest quality of reproduction possible.

If pages are missing, contact the university which granted the degree.

Some pages may have indistinct print especially if the original pages were typed with a poor typewriter ribbon or if the university sent us an inferior photocopy.

Previously copyrighted materials (journal articles, published tests, etc.) are not filmed.

Reproduction in full or in part of this film is governed by the Canadian Copyright Act, R.S.C. 1970, c. C-30.

## AVIS

La qualité de cette microfiche dépend grandement de la qualité de la thèse soumise au microfilmage. Nous avons tout fait pour assurer une qualité supérieure de reproduction.

S'il manque des pages, veuillez communiquer avec l'université qui a conféré le grade.

La qualité d'impression de certaines pages peut laisser à désirer, surtout si les pages originales ont été dactylographiées à l'aide d'un ruban usé ou si l'université nous a fait parvenir une photocopie de qualité inférieure.

Les documents qui font déjà l'objet d'un droit d'auteur (articles de revue, examens publiés, etc.) ne sont pas microfilmés.

La reproduction, même partielle, de ce microfilm est soumise à la Loi canadienne sur le droit d'auteur, SRC 1970, c. C-30.

**THIS DISSERTATION HAS BEEN MICROFILMED EXACTLY AS RECEIVED**

**LA THÈSE A ÉTÉ MICROFILMÉE TELLE QUE NOUS L'AVONS REÇUE**

NL-339 (r. 86/06)

Canada

THE UNIVERSITY OF ALBERTA

# AN EXPLORATION OF VARIOUS ASPECTS OF ICE ACCRETION USING A SIMPLE CYLINDER ICING MODEL

by

WEIWEI JIANG

A THESIS

SUBMITTED TO THE FACULTY OF GRADUATE STUDIES AND RESEARCH

IN PARTIAL FULFILMENT OF THE REQUIREMENTS FOR THE DEGREE

OF MASTER OF SCIENCE

IN

METEOROLOGY

DEPARTMENT OF GEOGRAPHY

EDMONTON, ALBERTA

SPRING, 1987

Permission has been granted to the National Library of Canada to microfilm this thesis and to lend or sell copies of the film.

The author (copyright owner) has reserved other publication rights, and neither the thesis nor extensive extracts from it may be printed or otherwise reproduced without his/her written permission.

L'autorisation a été accordée à la Bibliothèque nationale du Canada de microfilmer cette thèse et de prêter ou de vendre des exemplaires du film.

L'auteur (titulaire du droit d'auteur) se réserve les autres droits de publication; ni la thèse ni de longs extraits de celle-ci ne doivent être imprimés ou autrement reproduits sans son autorisation écrite.

ISBN 0-315-37760-7

THE UNIVERSITY OF ALBERTA

**RELEASE FORM**

NAME OF AUTHOR WEIWEI JIANG

TITLE OF THESIS AN EXPLORATION OF VARIOUS ASPECTS OF ICE ACCRETION USING A SIMPLE CYLINDER ICING MODEL

DEGREE FOR WHICH THESIS WAS PRESENTED MASTER OF SCIENCE

YEAR THIS DEGREE GRANTED SPRING, 1987

Permission is hereby granted to THE UNIVERSITY OF ALBERTA LIBRARY to reproduce single copies of this thesis and to lend or sell such copies for private, scholarly or scientific research purposes only.

The author reserves other publication rights, and neither the thesis nor extensive extracts from it may be printed or otherwise reproduced without the author's written permission.

(SIGNED) Weiwei Jiang

PERMANENT ADDRESS:

c/o Dr. Zuoning Jiang
An-Ding Hospital
Beijing, P. R. China

DATED March 19 1987

THE UNIVERSITY OF ALBERTA

FACULTY OF GRADUATE STUDIES AND RESEARCH

The undersigned certify that they have read, and recommend to the Faculty of Graduate Studies and Research, for acceptance, a thesis entitled AN EXPLORATION OF VARIOUS ASPECTS OF ICE ACCRETION USING A SIMPLE CYLINDER ICING MODEL submitted by WEIWEI JIANG in partial fulfilment of the requirements for the degree of MASTER OF SCIENCE in METEOROLOGY.

Edward Rawson

Supervisor

E.M. Yates

E. Reinelt

Date March 19, 1987

DEDICATED TO

My parents,

whose love and encouragement over the years

have made this work possible.

## ABSTRACT

Marine icing is hazardous and inconvenient for many types of maritime vessels and structures. Atmospheric ice accretion on wires is one of the major problems in planning and constructing power transmission lines and communication networks in regions where freezing temperatures occur frequently. Apart from these overall dynamic effects, ice accretion can also be a hazard in numerous other ways.

An exploration of various aspects of ice accretion using the simple cylinder icing model was made. The sensitivities of various physical and environmental parameters were examined with the model. Calculations were presented of the relative contributions of heat exchange by conduction and convection, by evaporation and by the supercooling of accreted ice to the total heat exchange of growing cylindrical ice deposits. They revealed the regions of dominance of the different ratios for various icing conditions in ice accretion.

In this icing model, a potential airflow was assumed and the droplet trajectories were calculated in order to determine the collision efficiency of the icing object. A heat balance equation for the accreted ice surface was solved to obtain the freezing fraction. Finally, the wind velocity and liquid water content, being a function of height in the marine boundary layer, were used to simulate the ice accretion on a marine structure. A wind direction of 45° to the icing cylinder was assumed and various physical parameters of ice accretion during icing were used. The model results showed that under icing conditions, 7 metres above the sea surface, the icing processes are in the wet-growth regime. The icing intensities at heights lower than 7m decrease drastically at the beginning of the icing process, because of the rapid increase in ice deposit diameters. The freezing fraction decreases a little at first, then increases again. The icing rate is very sensitive to the liquid water content. The icing rates always increase during the icing processes under severe icing conditions. In the case study, the collision efficiency of the icing object was always high. The density of the ice deposit was high and constant.

## ACKNOWLEDGEMENTS

I wish to give my sincere thanks to my supervisor Dr. Edward Lozowski. It is his valuable guidance and perceptive advice that have enabled me to accomplish my study. I am grateful for his carefully and patient reading of the draft of this thesis. The financial support in the form of Researching Assistantship from Dr. Lozowski for my two years study is sincerely appreciated.

I wish to thank Dr. Ted Gates for his expert help as one of the leaders of the Icing Group and serving on my examination committee.

I wish to thank Dr. Erhard Reinelt for his kindness, his guidance of my study and for serving on my examination committee.

Also, I wish to thank all the friendly people in the Meteorology Division. It is their friendship and warm help that gave me a very good time while I studied here in the past two years. It is especially worth cherishing for a foreign student.

Finally, to Hao Zhang, my husband, I feel very much indebted for all his understanding and all the support he gave me.

## Table of Contents


| Chapter | | Page |
|---|---|---|
| 1. | INTRODUCTION | 1 |
| | 1.1 THE NATURE OF THE ICING PROBLEM | 1 |
| | 1.2 ICING MODELS | 3 |
| | 1.3 THE TASK OF AN ICING MODEL | 4 |
| 2. | DESCRIPTION OF THE ICING MODEL | 7 |
| | 2.1 CALCULATION OF THE ICING INTENSITY | 7 |
| | 2.2 THE ANGLE BETWEEN THE WIND DIRECTION AND THE CYLINDER AXIS | 9 |
| | 2.3 COLLISION EFFICIENCY | 10 |
| | 2.4 FREEZING FRACTION | 14 |
| | 2.5 WIND SPEED | 19 |
| | 2.6 LIQUID WATER CONTENT | 22 |
| 3. | MODEL RESULTS | 26 |
| | 3.1 HEAT TRANSFER RATIOS | 26 |
| | 3.1.1 DEFINING OF THE HEAT TRANSFER RATIOS | 26 |
| | 3.1.2 SOME RESULTS | 28 |
| | 3.2 TESTING THE SENSITIVITY OF THE COLLISION EFFICIENCY TO DROPLET AND CYLINDER DIAMETERS | 31 |
| | 3.3 TESTING THE SENSITIVITY OF ICING INTENSITY TO THE WIND SPEED AND AIR TEMPERATURE | 31 |
| | 3.4 AN APPLICATION OF THE CYLINDER ICING MODEL TO MARINE STRUCTURES | 35 |
| 4. | DISCUSSION OF RESULTS | 47 |
| | 4.1 THE HEAT EXCHANGE RATIOS | 47 |
| | 4.2 THE COLLISION EFFICIENCY | 48 |
| | 4.3 MODEL APPLICATION TO PREDICT ICE LOAD ON MARINE STRUCTURE | 48 |

4.3.1 THE FREEZING FRACTION ..... 48

4.3.2 THE DENSITY OF ACCRETED ICE ..... 49

4.3.3 THE ICING INTENSITY ..... 50

4.3.4 THE SENSITIVITY OF ICE LOAD TO ATMOSPHERIC PARAMETERS ..... 51

4.3.5 THE ASSUMPTIONS IN THIS MODEL ..... 51

4.3.6 APPLICATION OF THE ICING MODEL ..... 53

5. CONCLUSIONS ..... 55

Bibliography ..... 57

## LIST OF TABLE


Table | Page

Table 2.1 Constants of the fifth-degree polynomial in wind speed to compute the height of the wave. 25

Table 3.1 The parameters used in the marine icing model. 36

## LIST OF FIGURES


| Figure | Page |
|---|---|
| Fig.2.1 The angle between the wind direction and the cylinder axis. | 8 |
| Fig.2.2 The angle between two vectors with a common point. | 9 |
| Fig.2.3 Droplet trajectory in front of a cylinder in an airstream. | 13 |
| Fig.2.4 Wind speed profile over sea surface. | 21 |
| Fig.2.5 Liquid water content profile over sea surface. | 24 |
| Fig.3.1 Heat exchange ratios. | 30 |
| Fig.3.2 The sensitivity of the collision efficiency. | 33 |
| Fig.3.3 The sensitivity of the icing intensity. | 34 |
| Fig.3.4 An application of the simple cylinder icing model. | 35 |
| Fig.3.5 Ice load on the cylindrical marine structure. | 39 |
| Fig.3.6 The ice deposit diameters as a function of height and time. | 40 |
| Fig.3.7 The icing rate at different height as a function of time. | 41 |
| Fig.3.8 The icing intensity at different height as a function of time. | 42 |
| Fig.3.9 The change of the freezing fraction at different height as a function of time. | 43 |
| Fig.3.10 The sensitivity of ice load on the cylinder to the air temperature at two different times. | 44 |
| Fig.3.11 The sensitivity of the ice load on the cylinder to the droplet size at two different times. | 45 |
| Fig.3.12 The sensitivity of the ice load on the cylinder to the wind speed at two different times. | 46 |

# Chapter 1

# INTRODUCTION

## 1.1 THE NATURE OF THE ICING PROBLEM

Icing is a natural phenomenon that sometimes jeopardizes human lives. Like floods and tornados, it is one of the unavoidable phenomena of nature. However, in the history of mankind's struggle with nature, icing and its effects have been recognized and accepted as a natural phenomenon. This study is aimed at gaining knowledge of icing and at analyzing the physics of this phenomenon.

Icing can be of hazard in various ways. The most hazardous icing may be marine structure icing. The following are true stories: On 26th January 1955, the English trawlers *Lorella* and *Roderigo* overturned north-east of the Northen Cape of Iceland in freezing conditions during a storm in which 40 men died.[1] On 8th February 1959 the Icelandic steam trawler *Fuli* was lost with her entire crew on the Newfoundland Banks because of icing. At the same time a Canadian fishing vessel was lost off Newfoundland. The Icelandic steam trawler *Thorkell Mani* was within a hair's breadth of capsizing, and a number of other trawlers, including several German ones, struggled against the storm, drifting ice and, above all, heavy ice on board (Mertins, 1968).

In addition to the above disasters, icing on towers, buoys, automatic meteorological instruments, helicopter platforms and other structures causes many safety risks and inconveniences. Marine icing has been recognized as a serious problem for a long time and has been discussed in the scientific literature for more than one hundred years (Nature, 1881). During the past decade the need for deeper understanding of atmospheric icing in the marine environment has increased considerably as human activities, such as safety criteria and structural design required knowledge of the hazards caused by the arctic environment. More

[1]1. Hay,R.F.M. Meteorological aspects of the loss of *Lorella* and *Roderigo*. *Mar. Obsr., London*,26, No.172, 1956, pp. 89-94.
2. Rodewald, M. O. The end of *Roderigo* and *Lorella*. *Wetterlotse*, Hamburg, No. 84/85, March 1955,pp. 56-66.

recently, Minsk(1977), Stallabrass(1980), Horjen(1981), Makkonen(1984), Jessup(1985), Lozowski and Gates(1985), Brown and Roebber(1985) have all reviewed various aspects of this subject as well.

Ice can be built up because of supercooled fog, freezing rain or drizzle, falling snow, and spindrift. However, the principal and most serious cause of icing is the sea spray generated by the passage of a vessel through heavy seas when the air and sea surface temperatures are low. When ice builds up on the superstructure of a ship, the added mass of the accretion can lower the freeboard and raise the centre of gravity. This can be very dangerous and sometimes a ship becomes even unstable because of icing, to the extent that she capsizes too quickly to leave any survivors who could report on the catastrophe.

In addition, Makkonen(1984) reviewed the icing problems and pointed out that atmospheric ice accretion on wires is also a major problem in planning and constructing power transmission lines and communications networks in regions where freezing temperatures occur frequently. Damage to structures by ice loads causes huge economic losses and operational difficulties in the power industry.

An extreme icing episode has been reported by Bendel and Paton (1981). A severe ice storm devastated 23 counties in southern Wisconsin in March 1976. The deposited ice accumulations of more than 10 cm in some areas. Direct cost pertaining to damage directly attributable to ice accumulation, such as damage to lines caused by the falling of ice-laden tree limbs and to support structures of the $50.4 million in damages in the 23-county area, the electric utilities suffered losses of $13.7 million for equipment repair and damages.

Not involving directly the aforementioned dynamic effects, Lozowski and Gates(1986) have reviewed some other aspects of icing hazards. A coating of ice may immobilize important equipment such as doors, lifeboats, control devices and fire fighting equipment. Ice accretion on antennas and radomes can interfere with navigation and communication. Also, ice accretion can represent a hazard for helicopter, workboat, and supply vessel operations in the vicinity of marine structures.

As described by Lozowski et al. (1983), there is a need for models of the ice accretion process in several fields. The understanding and prediction of hail formation, power line icing, aircraft and marine icing are enhanced, if models are available to help analyze and organize the physics, and to assist with the practical estimation of icing effects. In other fields, the phenomenology of icing may be quite different because of differences in the geometry of the icing substrate, the sizes and chemical composition of the supercooled water droplets, ice crystals or snow, the ranges of liquid water content, air speed and the temperature involved. It is at present inconceivable that a single icing model could span the entire range of applications.

Models are used to investigate accreted ice in several fields of research for a number of specific purposes. The approach of present-day research is often directed towards practical applications, but also at times towards the basic interpretation of the physical properties of a material obtained in such a particular way as the impingement and freezing of supercooled water droplets. The goal of building icing models is to get the overall picture of the icing phenomena. It is, therefore, particularly challenging, because of the variety of purposes and the wide range of environmental conditions characterizing the different accretion processes.

## 1.2 ICING MODELS

According to Lozowski(1986), we may consider an icing model to be a mathematical device which allows us to predict ice accretion or to study the details of its occurrence, without having to perform experiments or to make the actual measurements. Icing models are used for various purposes, such as the real-time forecasting of icing, the calculation of extreme-value statistics for regulatory purposes, for improving the design of marine structures to limit icing effects, and for research into the details of the icing process.

There are two kinds of icing models: empirical models and physical models. The empirical models are those in which one observes a large number of icing events as well as their previous conditions, using statistical analysis to find out the most significant parameters for icing. The physical models are those in which a theoretical mathematical model is built, so

that one can simulate the intermediate steps, and understand the causal relationships between the input conditions and the output predictions.

There are a number of icing models which have been built and designed for the specific physical regimes of marine, transmission line and aircraft icing. For simplicity, most models have assumed cylindrical shapes. The reasons are threefold: first of all, cylindrical icing represents a simple, well-defined icing problem for which a solution can be used to help understand and predict icing in more complex situations; secondly, abundant knowledge of fluid dynamics for the flow around an cylinder already exists; and thirdly, it is easier to make comparisons among models. Models of a horizonal circular cylinder in a uniform cross-flow have been built by Makkonen (1984), Egelhofer et al. (1984), Horjen (1983), Lozowski, Stallabrass and Hearty (1983), McComber and Touzot (1981) and Macklin and Payne (1967). In the physical model category, the more difficult problem of accretion on airfoils has been treated by Gent and Cansdale (1985), MacArthur et al. (1982) and Oleskiw (1982). Some examples of empirical models in use are those developed by Mertins (1968), Comiskey et al. (1984) and Itagaki (1984).

All the modelers tried to cope with the uncertainties of the icing phenomenon under more or less the same physical assumptions, except for three aspects. They are: A. calculation of the collision efficiency as local or overall collision efficiency; B. treatment of the water film on the ice surface as a single or double interface; and C. prediction of the total ice or the detailed ice shape.

## 1.3 THE TASK OF AN ICING MODEL

Although icing models are different in many ways, the tasks of icing models are the same. Lozowski and Gates (1986) have reviewed various aspects of icing models and pointed out the three essential tasks for all icing simulation models. They are used to simulate: A. the amount of water which hits the icing object; B. the amount of water which freezes on the icing object; and C. the growth of the ice deposit. Let us consider each of these in turn.

*A. The Amount Which Impacts on The Icing Target:* To find the answer, Lozowski and Gates (1986) suggested that we characterize the droplet size and the liquid water content by considering the physics of the drop generation processes and then calculate the flux density of the water.

The droplets moving in the airstream are constrained by viscous drag forces, which make them tend to follow streamlines around the icing object. However, the inertia of the droplets causes their trajectories to deviate from the streamlines. Thus some of them strike the surface of the icing object. Therefore, one may ask how many droplets strike the icing target, or what the collision efficiency will be.

The water impingement rate is the product of the liquid water flux density and the cross-sectional area of the target. Lozowski and Gates (1986) defined the product of the flux density and the cross-sectional area as the potential impingement rate, and the ratio of the actual impingement rate to the potential impingement rate is known as the collision efficiency. One can either calculate the local and the total collision efficiencies. The difference between two collision efficiencies is that the impingement rate used is at a particular location on the cylinder or the impingement rate on the whole cylinder.

In icing models, a numerical calculation of the dimensionless equation of motion of a droplet in the airflow is usually made, so that the trajectory of the droplet is obtained. Based on this, the collision efficiency is calculated, which enables us to determine how much water impacts on the icing object. This has been done by Langmuir and Blodgett (1946) for droplets which are stationary with respect to the airstream far upstream of the accretion and for simple target geometries such as cylinders and plates placed normal to the airstream.

*B. The Amount Which Freezes:* The amount of water which freezes is determined by the rate at which the latent heat of freezing can be removed from the freezing interface. In most models this problem is addressed by considering the process to be stationary and formulating a heat flux balance (Lozowski et al. 1986). This balance includes the latent heat of freezing, the sensible heat of the impinging droplets which stick and of the shed water, convective sensible

and latent (evaporative) heat transfer with the airstream, and internal conduction. Although other heat transfer terms could be added to the list, the aforementioned are generally dominant terms (Lozowski,1986) . The solution of the stationary heat balance equation allows us to solve for the fraction of the impinging water which freezes (the freezing fraction). If the accretion is dry (the heat losses allow all of the impinging water to freeze), then the heat balance equation permits the determination of the deposit temperature. Non-stationary effects due to initial transients, spray pulsation, and varying environmental parameters either on short (turbulence) or long (synoptic) time scales are generally ignored (Lozowski et al. 1986).

*C. The Growth of the Ice Deposit:* It is an important application in an icing model to determine the ice accumulation over a long period of time. During the process of ice accretion on a structure, the dimensions of the ice deposit change with respect to time. The size change of an icing target induces other processes. First, the changed shape of the ice deposit affects the airflow, changes the collection area and, consequently, the amount of water which hits the icing target. Secondly, the increased size of the ice deposit changes the heat exchange and the amount of water which freezes.

The above-mentioned feedback effects can lead to continuous changes in various parameters, such as the collision efficiency, heat transfer and the density of the accreted ice (Lozowski, 1986). On this account, the numerical model integration must proceed in a stepwise fashion with respect to time.

## Chapter 2

## DESCRIPTION OF THE ICING MODEL

The model to be described in this thesis simulates the accretion of supercooled water droplets onto a single, slowly rotating, circular cylinder. It is based on Makkonen's (1984) icing model. The Makkonen model has been improved in two ways: first, unlike any other icing models, it is assumed that the accreting cylinder is arbitrarily oriented in the wind field; second, vertical changes of wind speed and liquid water content have been taken into account.

An exploration of various aspects of ice accretion using the simple cylinder icing model is made. The sensitivities of the collision efficiency and the icing intensity to atmospheric parameters are examined. Calculations are presented of the relative contributions of heat exchange by conduction, convection and evaporation to the total heat exchange of the growing cylindrical ice deposit. They reveal the regions of dominance of the different heat transfer components for various icing conditions.

### 2.1 CALCULATION OF THE ICING INTENSITY

Based on Makkonen's (1984) model, the icing intensity on a cylindrical object may be defined as the rate of increase in the mass of ice divided by the surface area of the ice deposit that faces the wind. If we assume that the wind blows in a direction normal to the cylinder axis, the icing intensity can be calculated from:

$$I^* = \frac{2}{\pi} E n v w \qquad (2.1)$$

where E is the overall collision efficiency, n is the freezing fraction, (the ratio of the icing intensity to the mass flow of the impinging water droplets), v is the wind speed and w is the liquid water content of the air.

If the wind direction is not normal to the cylinder, a wind direction of angle $\theta$ to the icing cylinder axis is assumed. Then the icing intensity is (Makkonen, private

communication):

$$I = I^{*}\sin\theta \qquad (2.2)$$

We define the $\theta$ angle as the angle between wind direction and the direction of the cylinder axis (Fig.2.2).

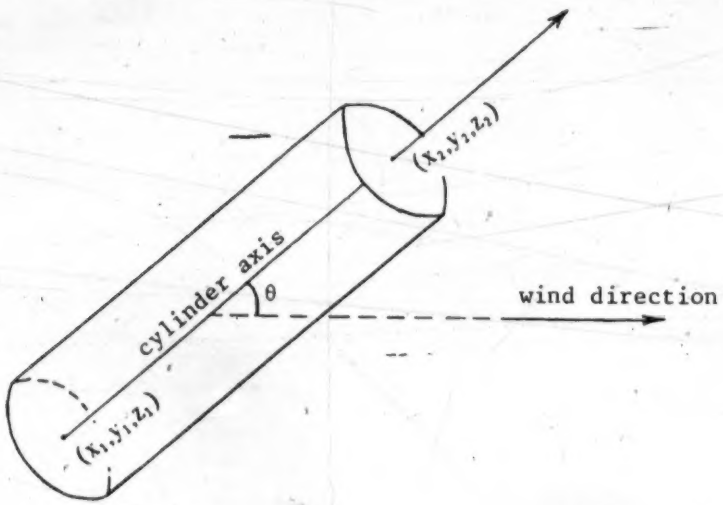


Fig.2.1 The angle between the wind speed and the cylinder axis.

The quantities I, E and n in Eq.(2.1) are the overall values for the icing object. In the model, the ice deposit is assumed to maintain a cylindrical form during the icing process due to the rotation or a slow change of the wind direction. This assumption simplifies the problem considerably. The actual accreted ice deposits on wires sometimes have an elliptical

form (Makkonen, 1984) . However, the deviation from a circular shape is not large for real icing cases, especially for transmission line icing. Observations on Mount Washington, New Hampshire (Howe, 1982), and from the USSR (Dranevic, 1971) show that the average ratio of the minor axis to major axis on actual power line conductors is 0.88 for glaze and 0.82 for rime.

## 2.2 THE ANGLE BETWEEN THE WIND DIRECTION AND THE CYLINDER AXIS

As we mentioned at the beginning of the chapter, in this model we assume that the accreting cylinder is arbitrarily oriented in the wind field. In view of the angle $\theta$ between the wind direction and the cylinder axis, the icing intensity is assumed to be reduced by $\sin\theta$, compared with the icing intensity for the wind normal to the cylinder axis.

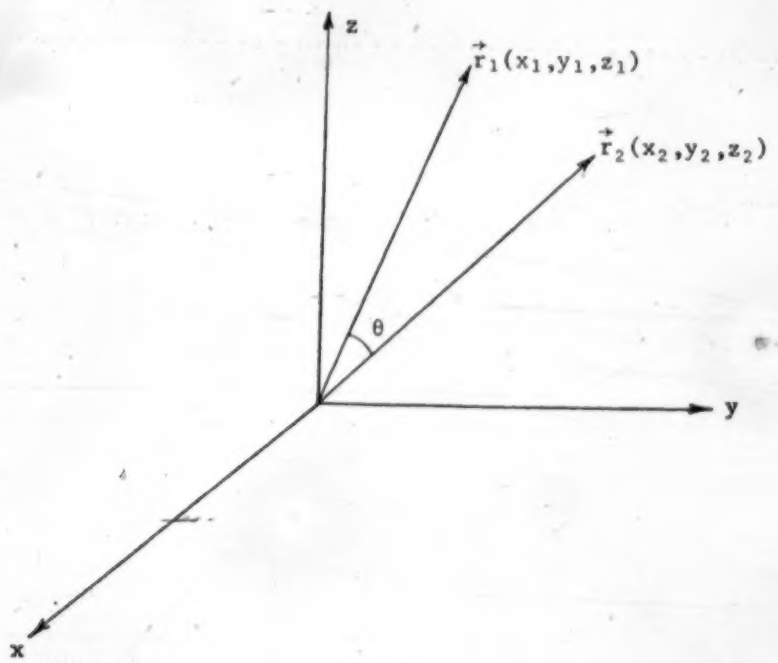


Fig.2.2.The angle between two vectors with a common point.

To calculate $\sin\theta$, we may find the angle between two lines with a common point first. Let the common point be the origin and establish vectors $\vec{r}_1=(x_1, y_1,z_1)$ and $\vec{r}_2 = (x_2,y_2,z_2)$ on the two lines (Fig.2.2).

Then $\vec{r}_1 \cdot \vec{r}_2 = |\vec{r}_1|\ |\vec{r}_2| \cos\theta$

Hence

$$\cos\theta = \frac{x_1x_2+y_1y_2+z_1z_2}{(x_1^2+y_1^2+z_1^2)^{1/2}(x_2^2+y_2^2+z_2^2)^{1/2}} \tag{2.3}$$

Now, we apply this to an arbitrarily oriented cylinder (Fig.2.2).

Moving the origin in Fig.2.2 to $(x_1,y_1,z_1)$, the vector along the cylinder axis is $[(x_2-x_1, y_2-y_1,z_2-z_1)]$. Without loss of generality, the wind vector can be assumed to lie along the y-axis so that a unit vector in this direction is (0,1,0). Using the above result yields:

$$\cos\theta = \frac{y_2-y_1}{[(x_2-x_1)^2+(y_2-y_1)^2+(z_2-z_1)^2]^{1/2}} \tag{2.4}$$

By using the relationship between $\sin\theta$ and $\cos\theta$ , we can easily calculate $\sin\theta$.

## 2.3 COLLISION EFFICIENCY

A water droplet moving in the airstream towards an icing object may follow streamlines around the icing object, or deviate from the airstream, then strike the icing object. Therefore, for the purpose of calculating the collision efficiency, we must calculate the droplet trajectories. Traditionally, a potential flow approximation for the airflow around the accreting object is assumed, and then the differential equation for the velocity potential is solved numerically.

This has been done by Langmuir and Blodgett (1946) for droplets which are stationary with respect to the airstream far upstream of the accretion, and for simple target geometries such as cylinders and plates placed normal to the airstream. The dimensionless equation of motion for spherical droplets around a cylinder is , according to Langmuir and

Blodgett (1946)

$$K\frac{dv'_d}{d\tau} = \frac{c_d Re_d}{24}(v'_a - v'_d) \qquad (2.5)$$

where $K$ = inertia parameter. $K = d^2\rho_w/9\mu D$.

$\tau$ = time [2]

$c_d$ = drag coefficient

$Re_d$ = droplet Reynolds number based on the droplet's velocity relative to the air

$(Re_d = d\,\rho_a\,|\,v_a - v_b\,|/\mu)$

$v'_a$ = dimensionless air velocity vector $v'_a = v_a/v$ [3]

$v'_d$ = dimensionless droplet velocity vector $v'_d = v_d/v$

$v_a$ = air velocity vector.

$v_d$ = droplet velocity vector.

$d$ = droplet diameter.

$\rho_w$ = water density.

$\mu$ = absolute viscosity of air.

$D$ = cylinder diameter.

$\rho_a$ = air density.

Calculating droplet trajectories requires numerical integration, which involves considerable computation time. However, the solution for E for a circular cylinder can be presented conveniently as a function of two dimensionless parameters K and $\phi$, where $\phi = 9\rho_a^2 D\,v/\mu\rho_w$.

[2] The dimensionless time $\tau$ is expressed in terms of c/v, as the unit of time. (c is the radius of the icing cylinder). This is the time that takes a particle to move a distance equal to the cylinder radius c, if travelling with the velocity v.

[3] The air moves with uniform velocity v, at a large distance from the cylinder.

BLANK PAGE INSERTED

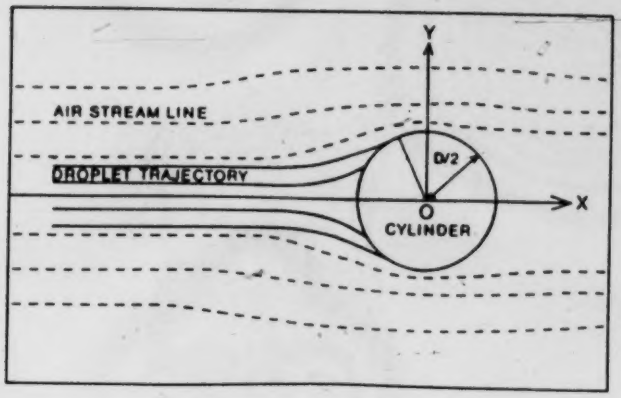


Fig.2.3 Droplet trajectories in front of a cylinder in an airstream.

Langmuir and Blodgett's (1946) calculation is one of the first published works for calculating the collision efficiency, and has long been the standard reference. Finstad (1986) challenged Langmuir and Blodgett's work. Instead of using the primitive analog computer, she used a digital computer to integrate the equation of motion. She replaced the drag coefficient formulation used by Langmuir and Blodgett (1946) with a more recent one, that of Beard and Pruppacher (1969). She has presented a new set of more accurate data to replace those of Langmuir and Blodgett, and has suggested the use of this more accurate data in future icing models. However, for consistency with the work of Makkonen (1984), we will continue to use the Langmuir and Blodgett's results.

The water droplet spectrum in the atmosphere and above the sea surface is not monodisperse, but has a certain droplet size distribution. Instead of calculating the collision efficiency for each droplet size, we can calculate the volume-weighted mean value for it. The task of computing volume-weighted average collision efficiency for a droplet size spectrum is often simplified by substituting a monodisperse size spectrum at the median volume diameter of the distribution. The collision efficiency of this monodisperse spectrum, $E_m$, can then be

corrected using the following empirical equation (Makkonen, 1984):

$$E = 0.69E_m^{0.67} + 0.31E_m^{1.67} \tag{2.6}$$

This formula gives a good estimate of the actual volume-weighted collision efficiency for a number of "typical" cloud droplet size spectra.

The formulae for calculating the overall collision efficiency $E_m$ are based on the tabulated results of Langmuir and Blodgett (1946). The following fits to their numerical data used in this model (Makkonen 1984) are:

$$E_m = 0.5[\log_{10}(8K_o)]^{1.6} \quad \text{for } K_o \leq 0.8 \tag{2.7}$$

$$E_m = K_o^{1.1}(K_o^{1.1} + 1.426)^{-1} \quad \text{for } K_o > 0.8 \tag{2.8}$$

where
$$K_o = K[0.087Re_d^{(0.76Re_d^{-0.027})} + 1]^{-1} \tag{2.9}$$

Eq.(2.9) is taken from Cansdale and McNaughtan (1977). Here K is the inertia parameter defined in Eq.(2.5) and $Re_d$ the droplet Reynolds number, based on the free-stream velocity also defined in Eq.(2.5).

## 2.4 FREEZING FRACTION

Freezing fraction, n, which appeared in the previous section, is the ratio of the icing intensity to the mass flux of the impinging water droplets. Ice growth is considered wet in the model when $n<1$, which means that there is some runoff from the ice deposit as a whole.

This runoff water is considered to be shed into the wind at the edges of the cylinder. In dry growth (n=1) there is no runoff from the deposit.

It has been explained in Chapter 1 that the freezing fraction can be calculated from the heat balance equation. Taking only the primary heat transfer processes acting on the icing surface into consideration, and assuming that the ice formation is a continuous steady-state process, an equilibrium heat balance at the ice surface may be formulated as follows (Makkonen 1984):

$$q_f + q_v + q_k + q_a = q_c + q_e + q_l + q_s + q_i \qquad (2.10)$$

where $q_f$ = latent heat released during freezing.

$q_v$ = frictional heating of air.

$q_k$ = kinetic energy of the impinging water.

$q_a$ = heat released in cooling the ice from its freezing temperature (0°C) to the surface temperature $t_s$.

$q_c$ = loss of sensible heat to the airstream by forced convection.

$q_e$ = evaporative heat loss to the airstream.

$q_l$ = heat loss in warming the impinging water to 0°C

$q_s$ = heat loss due to radiation.

$q_i$ = heat loss from the accretion due to internal conduction within the icing object.

The first term in Eq.(2.10) can be written as follows:

$$q_f = I l_f \qquad (2.11)$$

where I is the intensity of ice accretion (ice mass accreted per unit time and unit area) and $l_f$ is the specific latent heat of fusion. For the frictional heating of air;

$$q_v = (h\, r\, v^2)/(2\, c_p) \qquad (2.12)$$

where h = heat transfer coefficient.

r = recovery factor for viscous heating.

v = wind speed.

$c_p$ = specific heat of air at constant pressure.

The heat capacity of ice term is given by:

$$q_a = I\, c_i\, (0^{o}C - t_s) \qquad (2.13)$$

where $c_i$ is the average specific heat of ice between 0°C and $t_s$, and $t_s$ is the temperature of the surface.

The kinetic energy of the droplet $q_k$ can safely be neglected on stationary objects under natural atmospheric conditions (Makkonen 1984). For forced convection of sensible heat to the air:

$$q_c = h\, (t_s - t_a) \qquad (2.14)$$

where $t_s$ is the surface temperature (°C) and $t_a$ is the air temperature (°C). For the evaporative heat loss:

$$q_e = h\, k\, l_e\, (e_s - e_a)/(c_p p_a) \qquad (2.15)$$

where k = 0.69

$l_e$ = latent heat of evaporation

$e_s$ and $e_a$ = saturation vapor pressure over water at $t_s$ and $e_a$ actual vapor pressure in the air at $t_a$, respectively.

$p_a$ = free atmospheric pressure.

The heat transfer coefficient can be expressed in terms of the Nusselt number as $h = (K_a N_u)/D$. For the front half of the cylinder, Makkonen (1984) suggests the relation $N_u = 0.032 R_e^{0.85}$.

As Lozowski and Gates (1986) described, there are several items worthy of note. First, if the accretion is dry ($t_s < 0°C$), the use of latent heat of sublimation $l_s$ (instead of $l_e$) might be more appropriate. But in most of the marine icing cases, a film of water may exist on the accretion surface because of the finite time required for the impinging water to freeze completely. In this case, $l_s$ is used and $e_s$ will therefore be the saturation vapor pressure with respect to the water. In addition, $e_a$ may or may not be the saturation vapor pressure at the ambient air temperature $t_a$. For in cloud or in-fog icing we may safely make the assumption that the airstream is saturated. But for marine spray icing this may not be the case, although the most severe cases are likely to occur with a very large temperature differential between the air and the sea surface, in which case fog (Arctic smoke) may be formed.

For the heat loss in warming the impinging water to 0°C:

$$q_1 = \frac{2}{\pi} E v w \sin\theta c_w (0°C - t_a) \qquad (2.16)$$

where $c_w$ is the specific heat of water, and it is assumed that the temperature of the droplets in the free stream is the same as that of air. [4]

[4]The "$2/\pi$" is included, the water is intercepted by the cylinder cross-section, and then is assumed to be spread uniformly over the front face of the cylinder for the purpose of calculating the heat balance. Hence the ratio $2D/\pi D$, or $2/\pi$ is obtained. Once I has been calculated this way, however, the ice is assumed to be spread over the entire circumference of the cylinder.

The radiation budget at the surface can be estimated, as a first approximation, by neglecting the short-wave radiation and assuming that the emissivity of the salinity in the horizonal direction approaches one (Herman, 1980). Linearizing the equation for the difference in the emitted radiation of the icing surface, we obtain:

$$q_s = \sigma a (t_s - t_a) \tag{2.17}$$

where $\sigma$ is the Stefan-Boltzmann constant and $a = 8.1 \times 10^7 K^3$, assuming that the surface emissivity equals 1.

The conductive term $q_i$ is difficult to parameterize, since it depends on the thermodynamic properties of the object undergoing icing. The treatment here(Makkonen, 1984) is limited to the case where the conductivity of the structure is low, and the case where icing has been proceeding for a sufficient time for an icing deposit several centimeters thick to develop. In another words, the heat conductivity of ice is sufficiently low that $q_i$ on a cylindrical ice deposit can be neglected, except in the initial stage of icing where the thickness of the ice layer is only a few millimeters.

The relative magnitudes of the heat balance terms largely depend on the environmental conditions. In general $q_f$ is the major heat source term, and $q_c$ and $q_e$ are the dominant heat loss terms. However, $q_l$ becomes more important with increasing liquid water content, and $q_s$ with decreasing wind speed. The term $q_v$ can be neglected except when the wind speed is very high and the air temperature is close to 0°C.

Assuming the ice growth is wet, i.e. $t_s = 0$ and $e_s = e_0$, and putting all of the heat balance terms into the heat balance equation (Eq. 2.10) we can solve for the icing intensity:

$$I = h l_f^{-1}[-t_a + \frac{k l_e}{c_p p_a}(e_o - e_a) - \frac{r v^2}{2 c_p}] - l_f^{-1}(\frac{2}{\pi} E v w \sin\theta c_w + \sigma a) t_a \tag{2.18}$$

Once we have solved for I from (2.18), we can simply use Eq.(2.2):

$$n = I / (\frac{2}{\pi} E v w \sin\theta) \tag{2.19}$$

## 2.5 WIND SPEED

The logarithmic wind profile in the lowest 4-20m, fully turbulent, constant flux layer of the atmosphere is given by the Monin-Obukhov similarity analysis. Its integral form is:

$$U = U_0 + \frac{U_*}{\kappa} \ln \frac{Z}{Z_0} \tag{2.20}$$

where $U_0$ is the value of U at $Z_0$. $Z_0$ is called roughness length of the surface. In general it is a function of the geometry of the surface and of the length $\nu/U_*$, where $\nu$ is the kinematic viscosity of the air, $\kappa$ is the Von Karman constant ($\kappa=0.4$), and $U_*$ is the friction velocity.

To compute the wind speeds for the various altitudes it is convenient to refer all wind speed measurements to the level of 10m above the mean water level (Zakrzewski, 1986).

Then

$$U = U_{10} + \frac{U_*}{\kappa} \ln \frac{Z}{10} \tag{2.21}$$

The friction velocity can be formulated as:

$$U_* = U_{10} (C_{10})^{\frac{1}{2}} \tag{2.22}$$

where $C_{10}$ is the aerodynamic friction coefficient at a height of 10m. This variable depends on the 10m wind speed as was found by Smith (1980), who fitted his data with the following straight line:

$$10^3 C_{10} = 0.61 + 0.063 U_{10} \qquad (2.23)$$

The wind speed profile is plotted in Fig.2.4

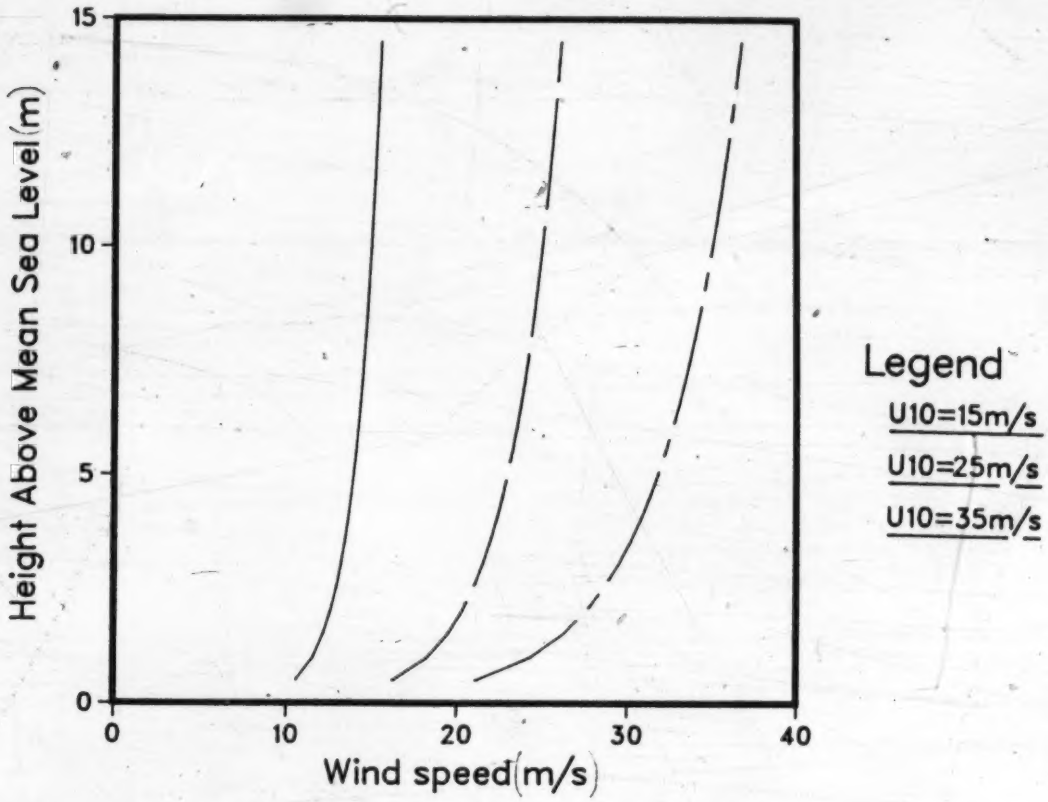


Fig.2.4 Vertical distribution of the wind speed over the sea surface. The wind speeds at each height are referred to the level of 10m above the mean sea level.

As we can see, the wind speed changes very little with respect to height above 3m. Therefore, for the sake of convenience, a constant wind speed will be used in the model in order to save computing time. For a wind speed lower than 5 meters or for rough seas, the logarithmic wind profile will be inappropriate (Wilson 1987, private communication). In such a case, the results in this layer need to be further verified.

## 2.6 LIQUID WATER CONTENT

In the model application, we will assume that w is a function of height in the marine boundary layer. Various people have tried to estimate the vertical distribution of the liquid water content above the sea surface with different degrees of sophistication(Horjen 1983a, Preobrazhenskii 1973, Jessup 1985, Itagaki 1984 and Stallabrass 1980). Lozowski et al. (1986) and Zakrzewski (1986) pointed out that of the two water sources: wind generated spray and wave generated spray, the latter is more important for marine structure icing. Thus, the liquid water content used in the model application for marine structure is based on the field experimental data gathered in the Sea of Japan by Borisenkov et al. (1975). Zakrzewski (1986) used the data and simulated the vertical profile of the wave-generated spray as follows

$$w = 6.1457 \times 10^{-5} H v_r^2 \exp(-0.55(z-3.01)) \quad (kg/m^3) \qquad (2.24)$$

Where H and $v_r$ are respectively the wave height and ship speed relative to the wave, z is height above the mean sea level. Zakrzewski (1986) has suggested that H is determined by the the fetch and wind speed at the 10m level. He gives the following empirical expression for H:

$$H(U_{10}) = B_0 + B_1 U_{10} + B_2 U_{10}^2 + B_3 U_{10}^3 + B_4 U_{10}^4 + B_5 U_{10}^5 \qquad (2.25)$$

where the constants $B_0$, $B_1$, $B_2$, $B_3$, $B_4$, $B_5$ are functions of fetch and are listed in Table 1 (Zakrzewski,1986). The component of ship speed perpendicular to an oncoming wave is given by the formula:

$$v_r = C_w - v_s \cos\alpha \quad (m/s) \tag{2.26}$$

There are two terms involved in the expression for the ship speed relative to an oncoming wave: the phase speed of the wave $C_w$, and the component of the ship speed along the normal to the wave, where $v_s$ is the ship speed, and $\alpha$ is the heading angle. [3] In this model, we have the intention to use this formula for a stationary structure, and so we assume the second term of the formula is zero.

The change of the liquid water content with height is shown in Fig.2.5. It is seen that the change of the liquid water with height is dramatic, especially at heights lower than 7 meters.

It is plausible to stop the ship at sea, treat it as a stationary structure and use Zakrzewski's liquid water content formula (1986). However, the mechanics of the wave-ship impaction and wave-structure impaction are totally different.

[3]The heading angle is the angle between the ship heading direction and the wind direction.

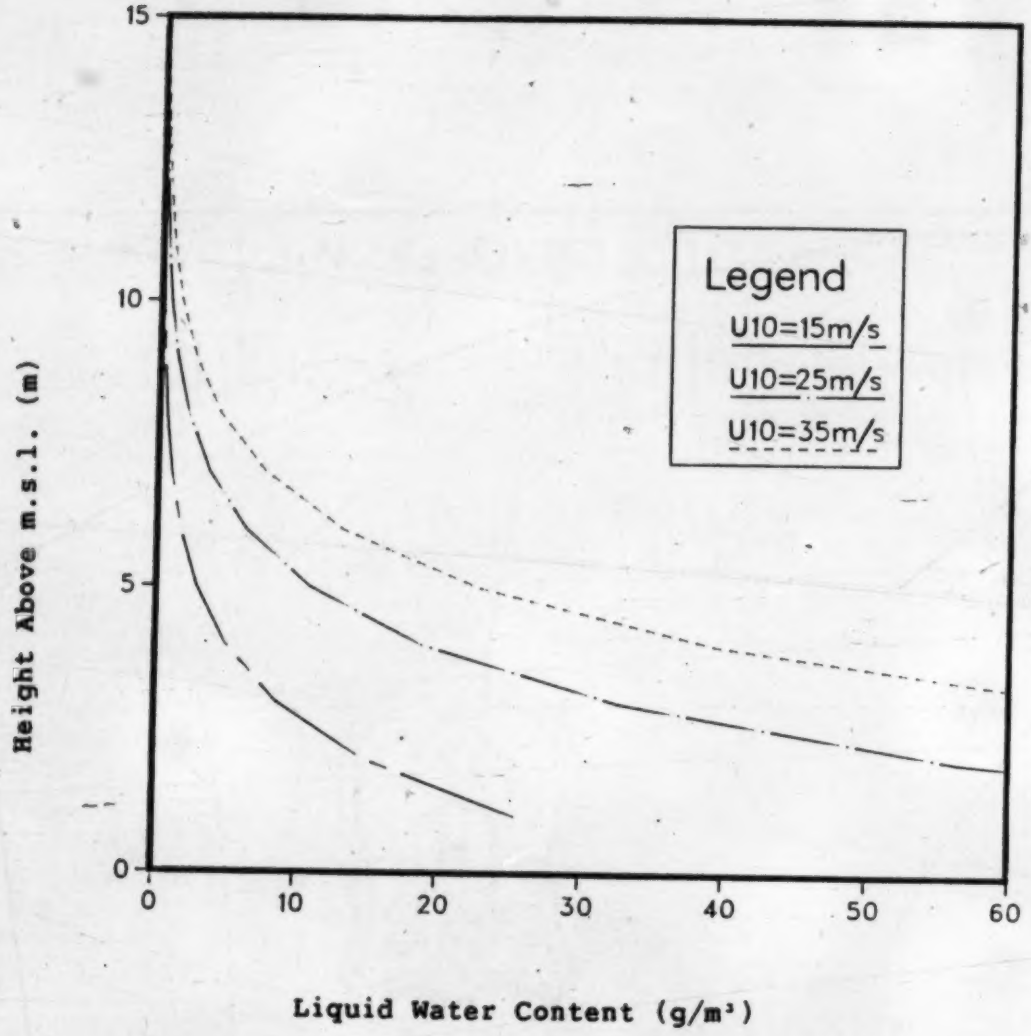


Fig.2.5 Example of the vertical distribution of liquid water content over the sea.

| FETCH(n.m.) | $B_0$ | $B_1$ | $B_2$ | $B_3$ | $B_4$ | $B_5$ |
|---|---|---|---|---|---|---|
| 100 | $8.68869 \times 10^{-1}$ | $-4.41178 \times 10^{-1}$ | $1.16227 \times 10^{-1}$ | $-7.87593 \times 10^{-3}$ | $2.62150 \times 10^{-4}$ | $-3.34401 \times 10^{-6}$ |
| 200 | $-7.71688 \times 10^{-1}$ | $2.71899 \times 10^{-1}$ | $1.07151 \times 10^{-2}$ | $-8.30642 \times 10^{-4}$ | $5.99481 \times 10^{-5}$ | $-1.20460 \times 10^{-6}$ |
| 300 | -2.31314 | $5.96961 \times 10^{-1}$ | $-1.71261 \times 10^{-3}$ | $-1.75501 \times 10^{-3}$ | $1.32954 \times 10^{-4}$ | $-2.40288 \times 10^{-6}$ |
| 400 | $4.86322 \times 10^{-1}$ | $-3.41913 \times 10^{-1}$ | $1.14635 \times 10^{-1}$ | $-8.51850 \times 10^{-3}$ | $3.24417 \times 10^{-4}$ | $-4.49695 \times 10^{-6}$ |
| 500 | $6.55261 \times 10^{-1}$ | $-3.78443 \times 10^{-1}$ | $1.11329 \times 10^{-1}$ | $-7.55389 \times 10^{-3}$ | $2.75507 \times 10^{-4}$ | $-3.75483 \times 10^{-6}$ |

Table 2.1 Constants of the fifth-degree polynomial in wind speed to compute the height of the wave.

# Chapter 3

# MODEL RESULTS

## 3.1 HEAT TRANSFER RATIOS

### 3.1.1 DEFINING OF THE HEAT TRANSFER RATIOS

One of the applications of the heat balance equation is to test the dominant heat transfer ratios. We define the heat transfer ratio as the ratio of individual heat exchange by a certain physical process to the total heat transfered. It represents the different contributions to the total heat exchange. The relative magnitudes of the heat balance terms largely depend on the environmental conditions. In general, the latent heat released during freezing is the major heat gain term, and the forced convective loss of sensible heat to the air and evaporative heat loss are the dominant heat loss terms. However, the heat required to warm the mass of water that freezes to 0°C becomes relatively more important with increasing liquid water content (Makkonen 1984). Also, heat loss due to radiation increases in relative importance with decreasing speed. Frictional heating by the air can be neglected except when the wind speed is very high and the air temperature is close to 0°C.

Theoretical calculations by Schuman (1938) and Ludlam (1958) assumed, and experiments by List (1960) confirmed in principle, that only three of these heat transfer components have to be considered for the description of the total heat exchange of a growing hailstone. In the same way, we will assume the total heat exchange of the growing ice deposit can be described by these three terms. They are 1) conduction and convection, 2) evaporation or sublimation, and 3) the heat required to warm (or cool) the impinging water flux and cool the resulting ice to the final surface temperature.

Let us consider a cylindrical growing ice deposit with a diameter D and surface temperature $t_s$ under the ambient conditions: air temperature $t_a$, impinging water droplet diameter d, wind speed v, and liquid water content w.

The heat exchange by conduction and convection is given by:

$$q_{cc} = h ( t_s - t_a ) \tag{3.1}$$

with h, the convective heat transfer coefficient.

The heat exchange by evaporation or sublimation is given by:

$$q_{es} = h \frac{K l_e}{c_p p_a} ( e_s - e_a ) \tag{3.2}$$

The heat exchange due to warming the supercooled water and cooling the ice is:

$$q_{cp} = \frac{2}{\pi} E v w (c_w t_a - n c_i t_s) \tag{3.3}$$

Where the $t_a$ and $t_s$ must be expressed in °C.

The sum of the components, $q_{cc}$, $q_{es}$, and $q_{cp}$, represents the total heat q transfered from the ice deposit surface per time unit. Under equilibrium conditions, this value equals the latent heat $q_f$ released by the partial or complete freezing of the accreted ice deposit given by:

$$q_f = \frac{2}{\pi} E v w l_f n \tag{3.4}$$

where $l_f$ is the specific latent heat of fusion at 0°C, n is freezing fraction.

Thus, under equilibrium conditions we get

$$q_{cc} + q_{es} + q_{cp} = q_f \tag{3.5}$$

Dividing by $q_f$ leads to:

$$\frac{q_{cc}}{q_f} + \frac{q_{es}}{q_f} + \frac{q_{cp}}{q_f} = 1 \tag{3.6}$$

or:

$$R_{cc/f} + R_{es/f} + R_{cp/f} = 1 \tag{3.7}$$

where $R_{cc/f}$ stands for $q_{cc}/q_f$ and so forth.

These three ratio represent the different contributions to the total heat exchange. Their values are:

$$R_{cc/f} = \frac{h\,(t_s - t_a)}{2/\pi\, E\, v\, w\, l_f\, n} \tag{3.8}$$

$$R_{es/f} = \frac{(h\, K\, l_e / c_p\, p_a)(e_s - e_a)}{(2/\pi)\, E\, v\, w\, l_f\, n} \tag{3.9}$$

$$R_{cp/f} = \frac{(c_w\, t_a - n\, c_i\, t_s)}{l_f\, n} \tag{3.10}$$

Only two of three ratios can be assumed to be independent, the third always being determined by Eq.(3.7).

### 3.1.2 SOME RESULTS

These three heat exchange ratios are displayed in Fig.3.1 for a typical set of conditions. We can clearly see that the graph is divided into two parts by a deposit temperature of 0°C and an ice content of n=1. Spongy ice is growing to the upper right of this line, whereas a rime ice deposit is formed under the conditions in the lower left part of this boundary. The fine background lines are the ice deposit surface temperature, $t_s$. They are

very close to the air temperature when the wind speed is low. Superposed are the ratios $R_{cc/f}$ and $R_{es/f}$ where the values of $R_{cp/f}$ can be obtained for each point from Eq.(3.7). In Fig.3.1, the liquid water content used was 0.8g/m$^3$, the droplet size d was 20$\mu$m and the diameter of the icing target was 5cm. Since there are three heat exchange ratios, if in the region where the value of a heat exchange ratio is greater than 0.33, we say that this heat exchange ratio is dominant in that region. It is clearly shown in Fig.3.1 that in the given conditions, the heat exchange by conduction and convection is dominant in most of the regions on the plot. When the air temperature increases, the heat exchanges by conduction/convection and evaporation/sublimation decrease and increase respectively. The wind speed has stronger influences upon the heat exchange by conduction/convection when deposit temperature is low. When the differential between the air temperature and deposit temperature increases, the heat exchange by conduction/convection increases; whereas, for the same reason, the differential of the vapor pressures ($e_s$ and $e_a$) increases, thus, the heat exchange by evaporation/sublimation increases.

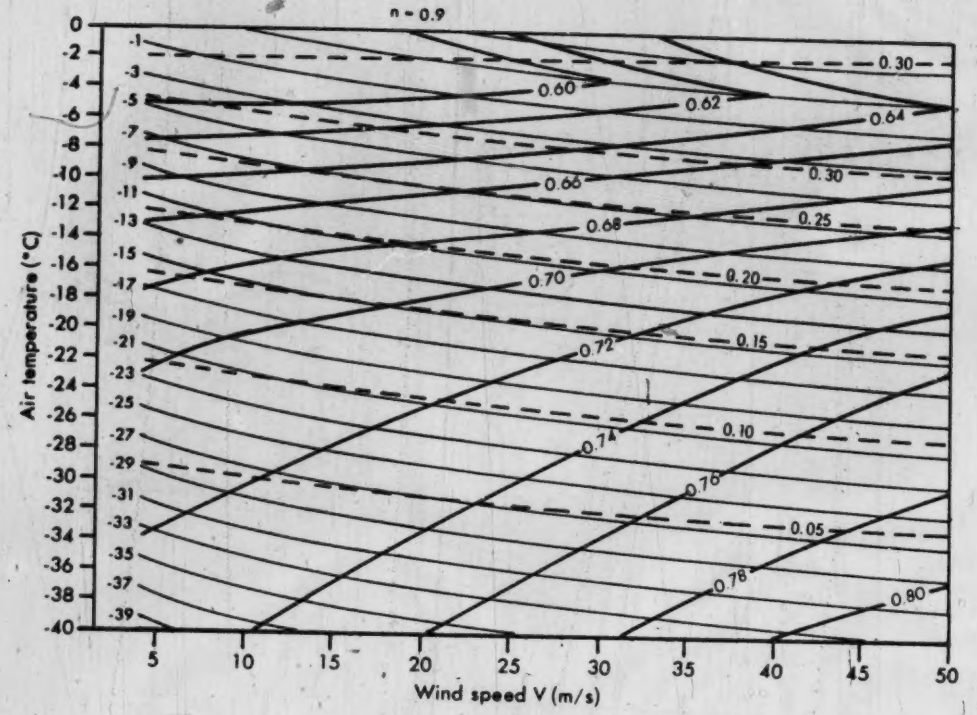


Fig.3.1 Contributions of the dominant heat transfer ratios for a cylindrical ice deposit. The fine background lines are the equilibrium surface temperature of the ice deposit. The dark solid lines are $R_{cc/f}$, the dashed lines are $R_{es/f}$. The parameters used were D=5cm, d=20$\mu$m, w=0.8g/m$^3$.

## 3.2 TESTING THE SENSITIVITY OF THE COLLISION EFFICIENCY TO DROPLET AND CYLINDER DIAMETERS

The sensitivity of the collision efficiency to both droplet diameter and the icing object diameter is shown in Fig.3.2. The behavior of the collision efficiency in Fig.3.2 shows it is a function of both droplet diameter and the icing object diameter. In Fig.3.2 the droplet sizes range from 1$\mu$m to 1000$\mu$m, including large droplet spectrum sizes. Logarithmic axes are used in order to include a broad range of both droplet diameters and icing object diameters, the latter ranging from 1cm to 10m. It is seen from Fig.3.2 that the collision efficiencies decrease with increasing cylinder diameter, and increase with increasing droplet diameter. The conditions used to plot the graph are air temperature $t_a = -10°C$, wind speed $v = 5m/s$.

It may be worth mentioning that the collision efficiency is not only a function of the two diameters, but also a function of wind speed. Makkonen (1984) showed that the collision efficiency increases with wind speed. In particular, it increases rapidly with the wind when the value of E is small.

## 3.3 TESTING THE SENSITIVITY OF ICING INTENSITY TO THE WIND SPEED AND AIR TEMPERATURE

Icing intensity, being a function of air temperature and wind speed, has been calculated for air temperatures ranging from 0°C to -20°C, and for wind speeds ranging from 5m/s to 30m/s. The calculation was made for a 5cm-diameter cylinder, a liquid water content of 0.2g/m$^3$, and a droplet size of 25$\mu$m. Their relation is presented in Fig.3.3 It is seen that icing intensity increases with increasing wind speed and decreasing air temperature. When the air temperature is close to 0°C, icing intensity changes very little with respect to the wind speed; whereas at very low air temperature, the icing intensity seems to have closer correlation with wind speed. On the basis of sensitivity analysis, Lozowski and Gates (1986) suggested that we may follow in the footsteps of Stallabrass (1980) and Launiainen et al. (1983), and proposed a simple formula which incorporates simply the air temperature and wind speed. Such a relation might take the form:

$$\text{Icing intensity} = -C\, t_a\, v$$

where C is a constant. Brown and Roebber (1985) have shown that, surprisingly, such a simple relation actually correlates slightly better with Canadian East Coast trawler icing-data than either the Stallabrass (1980) or Kachurin et al. (1974) model.

Icing intensity is also function of other atmospheric parameters. It increases with increasing droplet diameter and decreasing icing target size because of the changes of the collision efficiency. Icing intensity may be affected by the liquid water content in the airstream, and by the angle of wind direction. Also, icing intensity can be affected by other physical parameters. In addition, Makkonen (1984) pointed out that two possible mechanisms may affect icing intensity. First, in marine icing conditions, some of the excess water on the deposit surface, instead of being shed, may be incorporated into the ice structure, giving a spongy ice deposit. Second, in atmospheric icing conditions, ice crystals mixed with supercooled water droplets may affect I.

In addition, Prodi et al. (1986) proposed a two-stage ice accretion hypothesis. By obtaining artificial accretions on rotating cylinders in a wind tunnel, in controlled laboratory conditions, it is observed that the ice deposit grows in two stages by the soaking and refreezing of a previously formed porous structure. The evidence that two-stage growth may be a frequent occurence is changing the criteria of ice accretion interpretation: it introduces new criteria based on specific calculation of physical parameters and suggests various modifications of the criteria currently adopted.

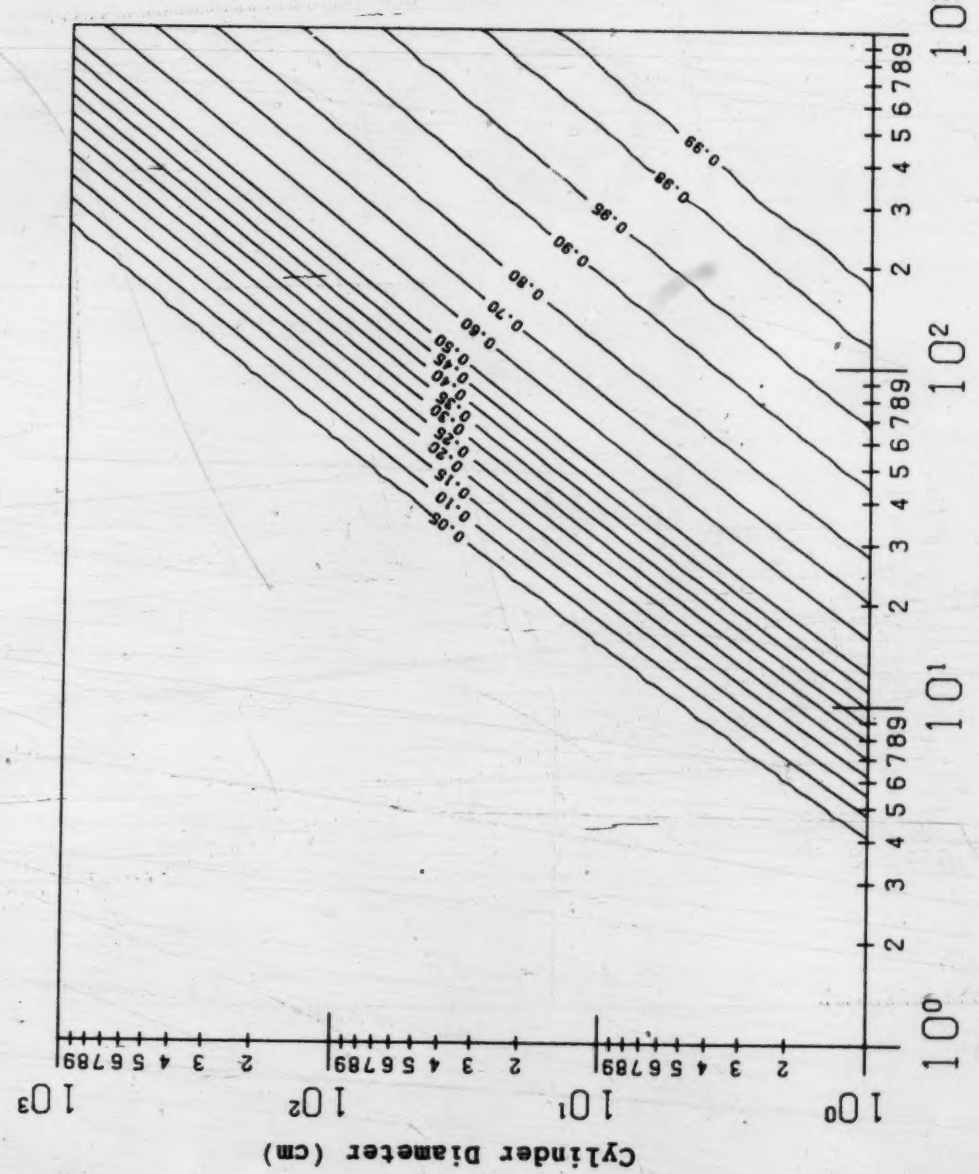


Fig.3.2 Sensitivity of the cylinder collision efficiency to variation in the droplet diameter and the icing object diameter. The parameters used were $t_a = -10^{0}C$, v=5m/s,

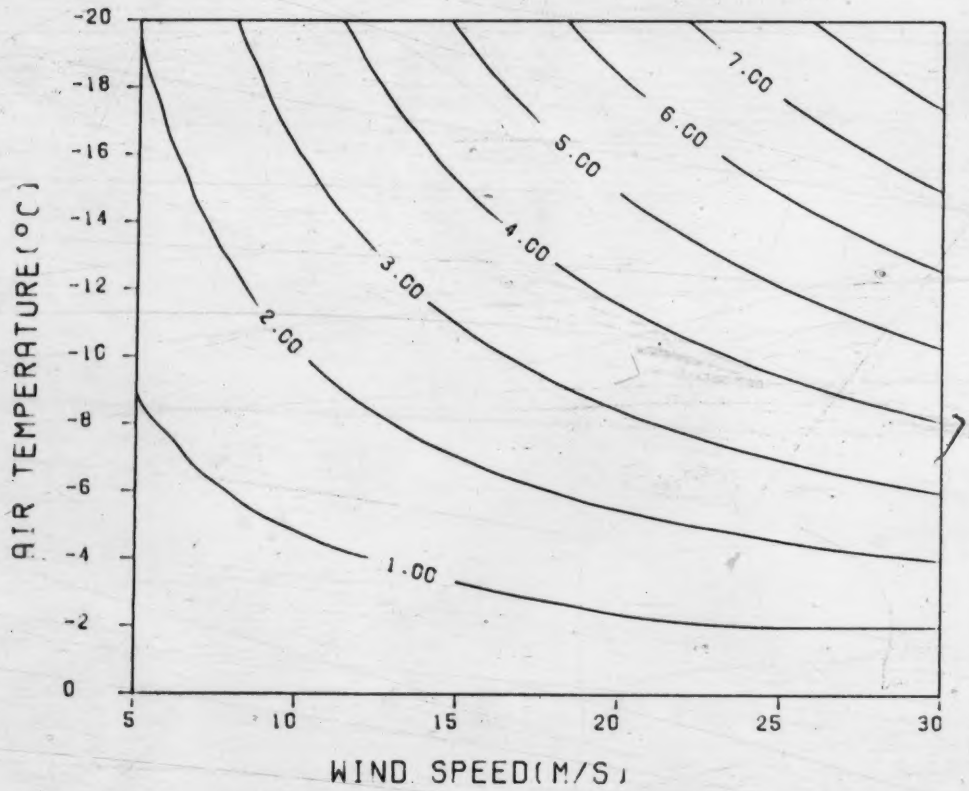


Fig.3.3 The test of sensitivity of the icing intensity to the wind speed and the air temperature. The parameters used were d=25$\mu$m, D=5cm and w=0.2g/m$^3$.

## 3.4 AN APPLICATION OF THE CYLINDER ICING MODEL TO MARINE STRUCTURES

A simple application of the single cylinder icing model to a marine structure is made. An example of the time-evolution of the quantities relevant to the icing process as simulated by the model is shown in Fig.3.5 - Fig.3.12. In this example, an angle of 45° between the wind direction and the cylinder axis is used (Fig.3.4). Other angles can be employed in the model.

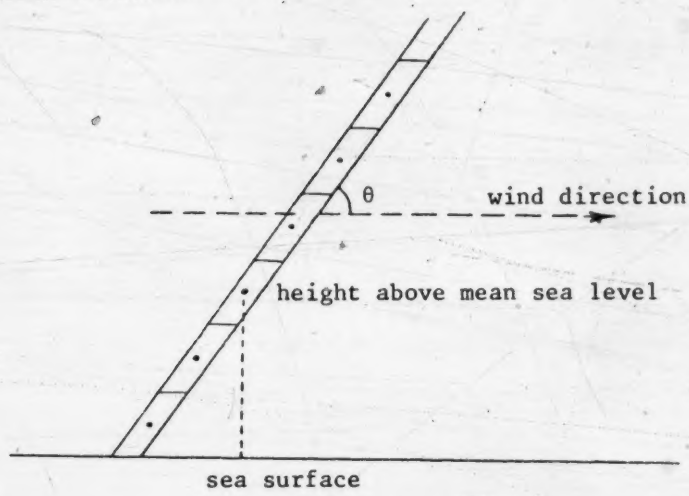


Fig.3.4 An application of the simple cylinder icing model on a cylindrical marine structure which is at a 45° angle to the wind direction.

| SYMBOL | DESCRIPTION | VALUE |
|---|---|---|
| $U_{10}$ | wind speed at 10m height | 15m/s |
| $t_a$ | air temperature | -8°C |
| v | wind speed | 15m/s |
| d | droplet diameter | 500$\mu$m |
| D | initial cylinder diameter | 1cm |

Table 3.1 The paramters used in the model application.

* constant v is used in the model rather than v(z) for simplicity.

We chose a cylinder to be the icing target because most of the marine structures are cylindrical objects, such as oil rigs, superstructures on ships and the like. And we assumed the cylinder is much longer than the distance that the sea spray can ever reach. However, only ice accretion on the cylinder due to sea spray was taken into account. For the purpose of testing the sensitivity to parameter variations of the ice accretion, the icing object was divided into sections, each one meter in length. The center point height of each section above the mean sea surface is assumed to be the height of that section in the model. The simulation of time dependence in the model is explained in appendix A.

Input parameters corresponding to rather severe icing condition were used in the simulation. All calculations were made for the parameters listed in Table 2. The time step used here is one hour. The ice load M has been plotted with height from 3 meters to 16 meters in Fig.3.5. The six curves indicate 60-hour ice load situations. Each curve is drawn after ten hours icing. The ice deposit diameters have also been plotted for every 10 hours in Fig.3.6. The icing intensity decreases rapidly with time (Fig.3.8), especially in the beginning of the icing process in the lower several meters of the cylindrical structure, due to the rapid relative increase in the deposit diameter and large liquid water content in the air. It shows that the ice growth is always in the wet regime below 7 meters. The freezing fraction, n, changed very little with time at each height. It decreases at first with time, and increases again, reaching 1 when the height of the section reaches h=7m.

Under such severe icing conditions, the ice load on the cylindrical structure exceeds 80kg/m after 10 hours of icing at a height of 3 meters. The thickness of the ice deposit is about 15cm, and the ice deposit density is 920kg/m$^3$. It is calculated that the ice deposit density in this case is not only high, but also a constant ($\rho$=920kg/m$^3$) even after 100 hours of icing. It might be caused by the large droplet size and the large impact velocity.

The ice load growth rates are shown as functions of time in Fig.3.7. The six curves represent six different heights on the cylinder. It is apparent that the icing rate is higher on the lower part of the cylinder. On the other hand, it is obvious that at 7m the icing processes change from wet to dry. Correspondingly, the icing rates have a drastic change in slope at 7m

as well. It is seen that after 60 hours icing, ice mass still accumulates.

Curves of the ice load for different values of the atmospheric parameters are shown in Fig.3.10 - Fig.3.12 Fig.3.10 shows that the ice loads are sensitive to the air temperature at wet growth condition (lower than 7m). The sensitivity of ice load to the median droplet diameter d in Fig.3.11 is high for both dry and wet growth processes. The strong influence of wind speed on the ice load in both wet and dry growth conditions is shown in Fig.3.12. The figure shows that the ice load is sensitive to the wind speed in both dry and wet growth conditions.

The calculation shows that the ice load change with the angle $\theta$; at any height, has its largest value for the wind blowing directly along the cylindrical structure normal, and drops by 23% and 71% for the wind direction 30° and 60°, respectively, away from the cylinder axis.

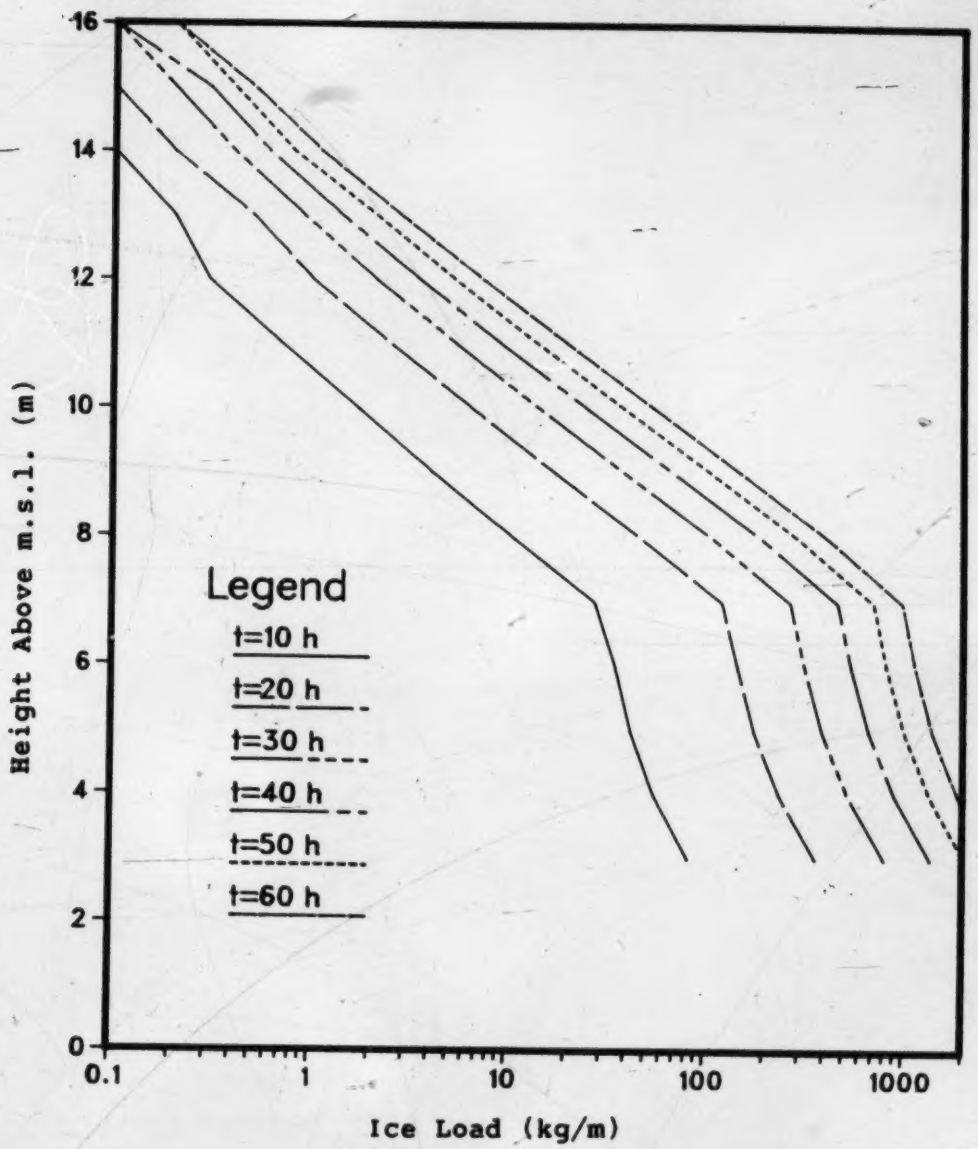


Fig.3.5 Ice load on the cylindrical marine structure as a function of height and time. The parameters used were those in Table 2.

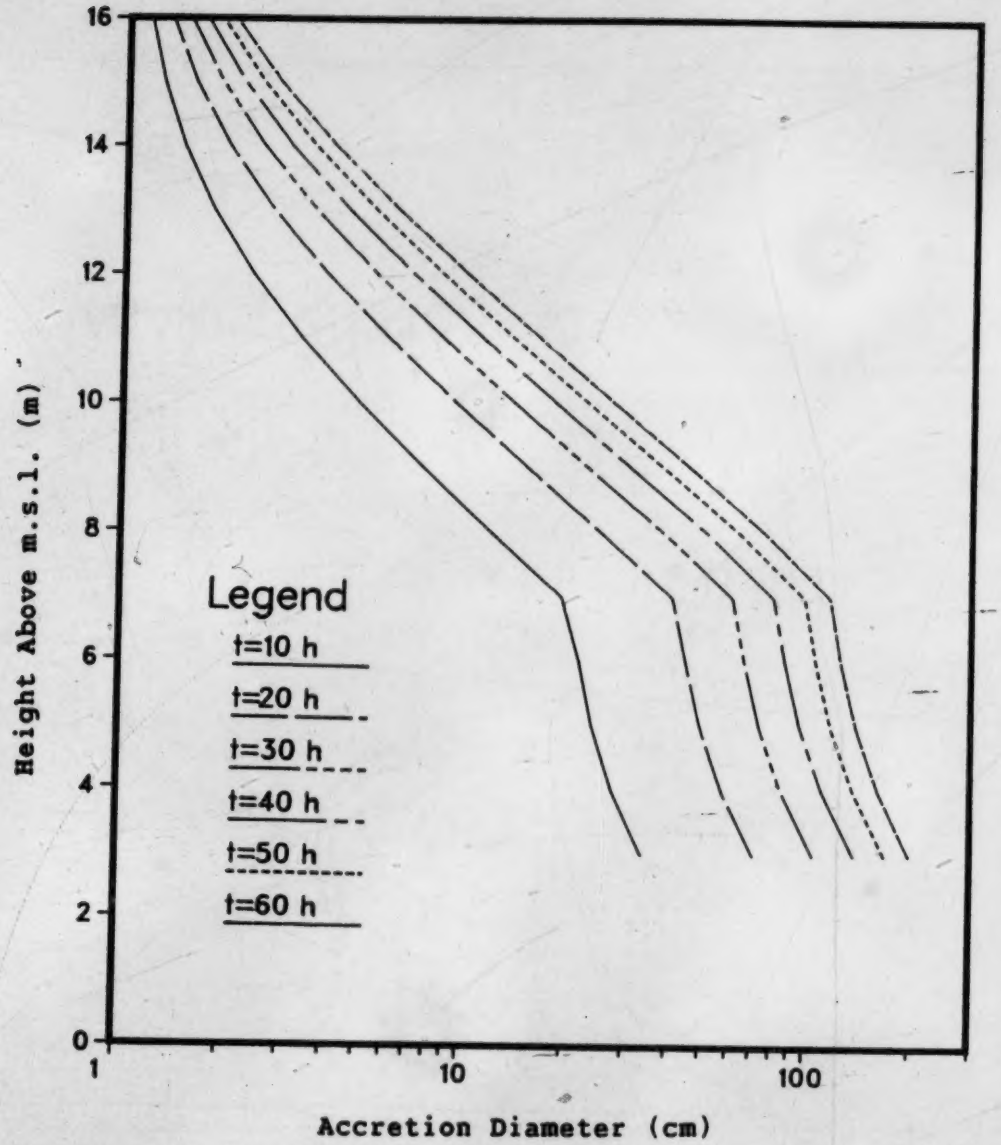


Fig.3.6 The ice deposit diameters as a function of height and time. The parameters used were those in Table 2. The liquid water content is described in Eq.(2.24).

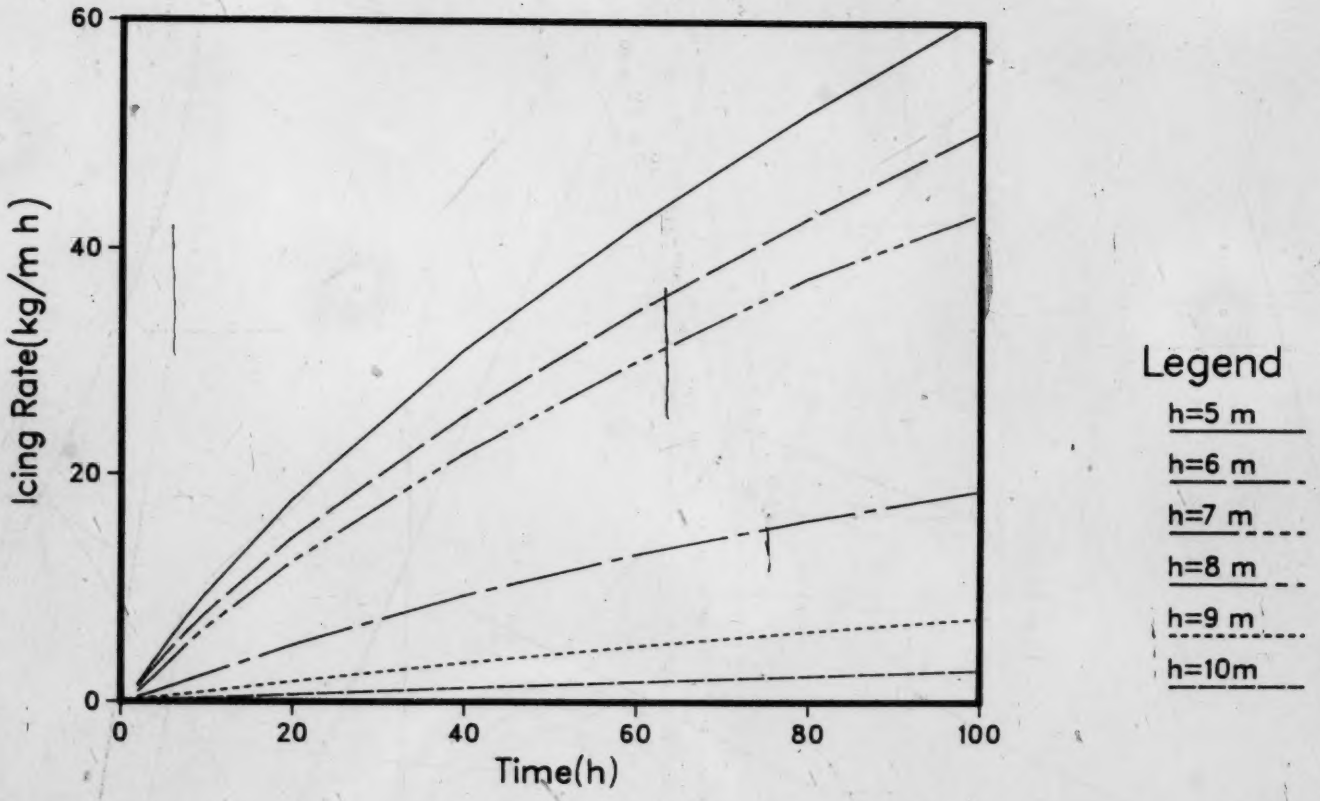


Fig.3.7 The icing rates as function of time. The icing rates for six different heights are also presented with six different curves. The parameters used were $U_{10}$=15m/s, $t_a$= -8°C, V=15m/s, d=500$\mu$m and D=1cm. The liquid water content is a function of height.

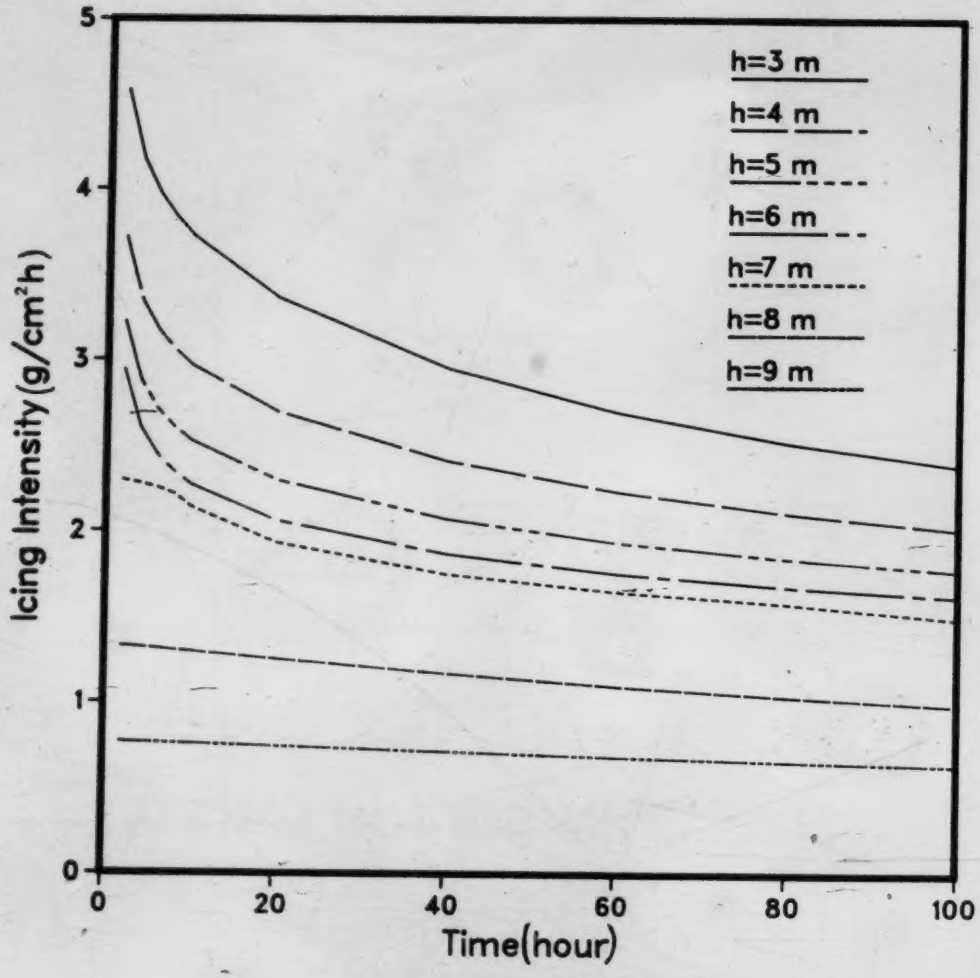


Fig.3.8 The icing intensities as a function of time at different heights. The parameters used were those in Table 2. The liquid water content is a function of height.

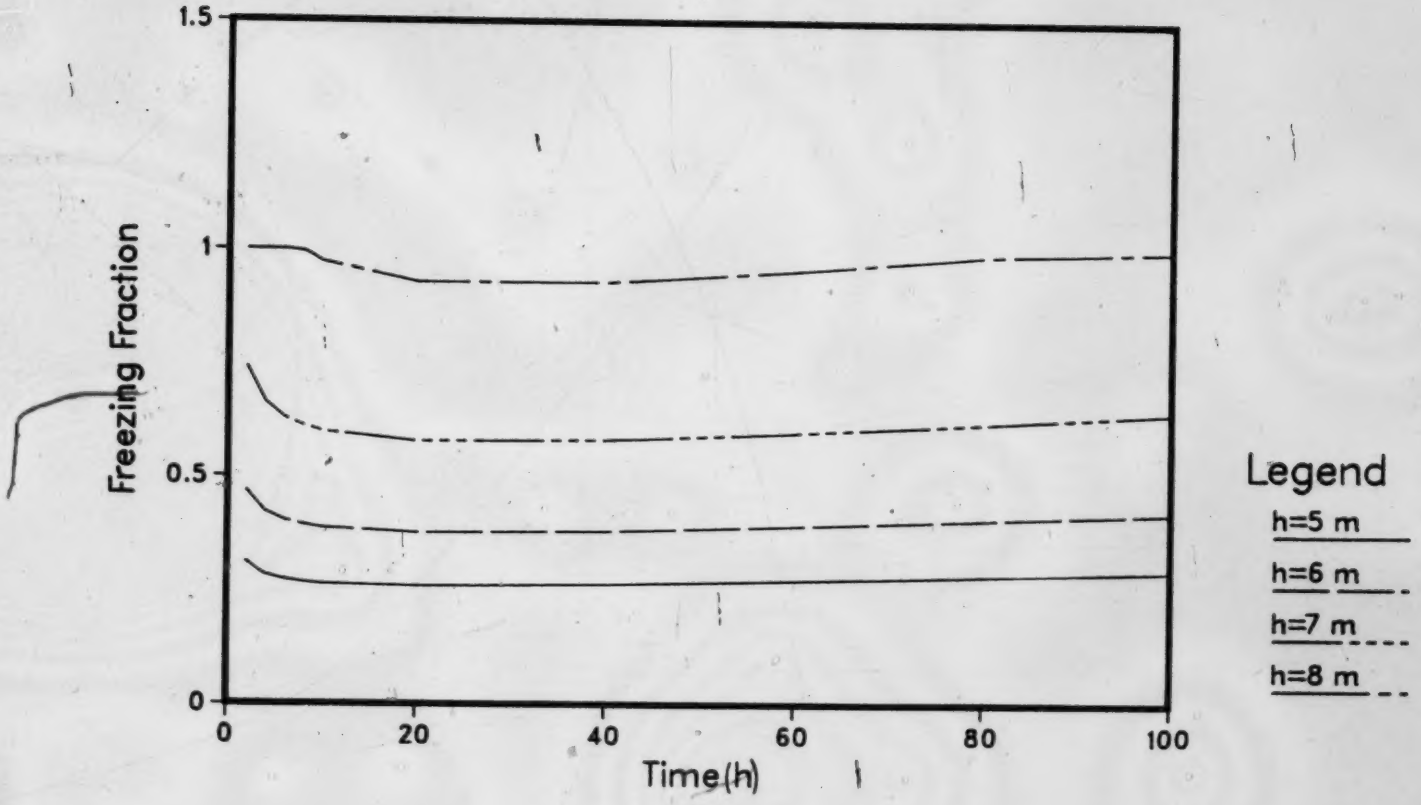


Fig.3.9 The changes of the freezing fraction with time at different heights in wet growth are shown here. The parameters used were those in Table 2. The liquid water content is a function of time.

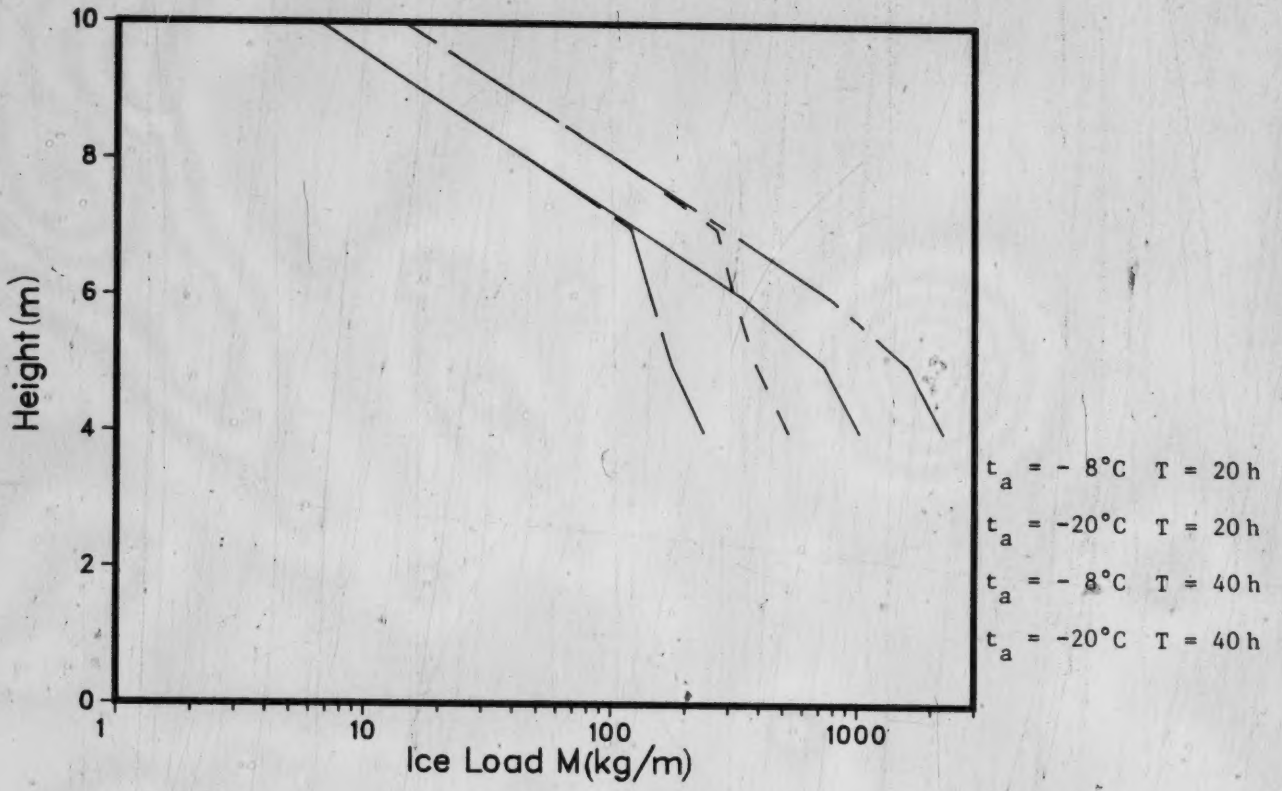


Fig.3.10 The sensitivity of the ice load on the cylinder to the air temperature at two different times. The air temperatures used were $t_a$ = -20°C, $t_a$ = -8°C. T=20 hours and T=40 hours respectively. The other parametefs used were given in Table 2.

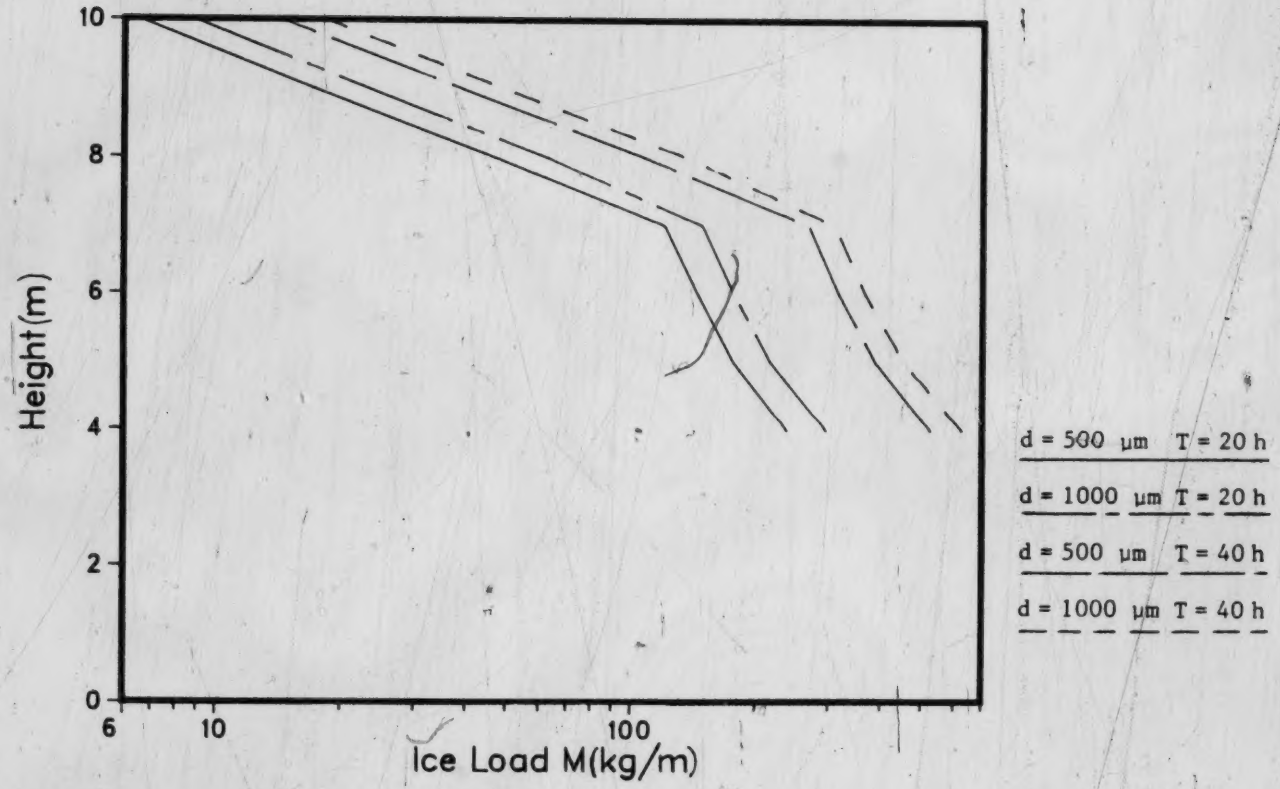


Fig.3.11 The sensitivity of the ice load on the cylinder to the median volume droplet diameter d=500$\mu$m and 1000$\mu$m at T=20 hours and T=40 hours. The liquid water content is a function of height. Other parameters used were given in Table 2.

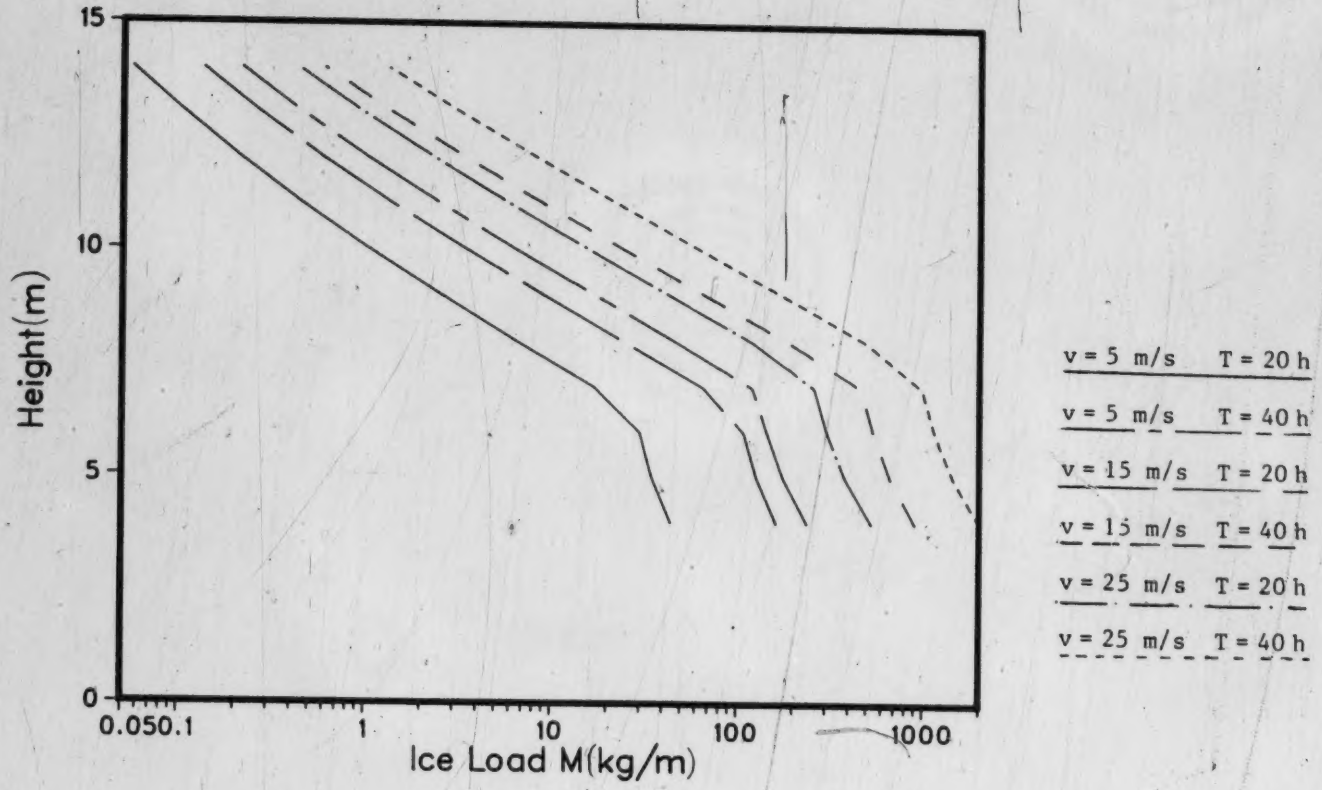


Fig.3.12 The sensitivity of the ice load on the cylinder to the wind speed at two different times.

## Chapter 4

## DISCUSSION OF RESULTS

### 4.1 THE HEAT EXCHANGE RATIOS

Theoretical calculations have been made for the three dominant heat exchange ratios at the ice deposit surface. These dominant exchange ratios are determined as a function of wind speed and air temperature of icing condition. The three heat transfer ratios are displayed in Fig.2.5. It is obvious that: the contribution of the heat exchange by conduction and convection is steadily increasing with increasing wind speed; the influence of evaporation is increasing with increasing ice deposit surface temperature, and has its highest value at a temperature near 0°C; the influence of the heat exchange by conduction and convection plays an important role when the ice deposit temperature is low. Also, all curves of equal ratios change their slope on passing through the zero-degree surface temperature.

From the testing results, only heat exchanges due to convection/conduction and sublimation/evaporation, respectively, seemed important; but in the light of icing conditions, it is possible that the heat exchange due to temperature differences between the impact droplet and the ice deposit surface is dominant in the important region where spongy ice is formed with relatively big droplets.

These heat exchange ratios are also considered to represent new parameters for further study about the relationship between icing conditions and the resulting ice deposit. Under the guidance of the theoretical calculation, the dominant heat transfer ratios can be simulated in icing experiments. Instead of using liquid water content, wind speed, collision efficiency, and icing intensity ete., the use of the heat transfer ratios as a new set of parameters to describe the icing conditions may be more satisfactory.

## 4.2 THE COLLISION EFFICIENCY

In Chapter 3 , we have seen the dependence of collision efficiency on the droplet size, the diameter of the icing object, and the wind speed. In fact, the air temperature also has an effect on collision efficiencies, because air density and the absolute viscosity of air depend on the air temperature, but this effect is negligible in practical applications (Makkonen 1984). Whether the water droplets flying in the airstream will impact on the icing object or not depends upon the values of the viscous drag forces and the inertia of the droplets. Having more inertia, when the bigger size droplets tend to deviate from the airstream, they are already in the immediate vicinity of the collecting object. Thus they have more chance to strike the collecting object. On the other hand, the acceleration of a water droplet is inversely proportional to the inertia parameter K (Eq.2.5), or in other words, it is proportional to the diameter of the icing object. So that for larger icing cylinders the droplets have more chance to get away from the icing object, the collision efficiencies decrease with respect to larger icing object.

Langmuir and Blodgett (1946) showed that when the interia parameter $K=1/8$, the corresponding collision efficiency $E=0$. We have used this in the model, but Makkonen (1984) has pointed out that $E=0$ may not be fully applicable to the real world, where the airflow is turbulent and the droplets are not of uniform diameter. Also, since E is sensitive to the object dimensions, ice may sometimes accrete locally on the icing object and form rime features, even though $E=0$ for the object as a whole.

## 4.3 MODEL APPLICATION TO PREDICT ICE LOAD ON MARINE STRUCTURE

### 4.3.1 THE FREEZING FRACTION

The parameters of air temperature, wind speed and liquid water content used in this example make the icing process a wet growth one for the height below 7m (Fig.3.9). The freezing fraction is less then unity below 7m, It decreases at first with respect to time, then increases again. From the model calculations, it appears that at the beginning of the icing

process, the collision efficiency is high, and it decreases more slowly than the convective heat transfer coefficient h (Eq.(2.19)). Correspondingly, n decreases slightly. After a period of time, the value of the collision efficiency drops rapidly, decreasing faster than h. Consequently, value of n increases again.

### 4.3.2 THE DENSITY OF ACCRETED ICE

The density of the glaze ice deposit is constant and always high ($\rho_i$=920kg/m). It might be produced due to high surface temperature and large drop sizes. The impingement of huge amounts of sea spray leads to slow freezing with significant spreading or flattening of the drops. Laboratory tests (Prodi et al. 1986) showed this kind of ice deposit usually have high density and no large gaps in the ice structure.

From the model calculation of the air temperature -8°C, the surface temperature of the ice deposit is always 0°C below 7m. [6] That is because in the lower part of the cylindrical structure, the liquid water content is so high that the contribution of the latent heat of freezing increases, and this is only partly made up by a compensating increase in the sensible heat required to warm the accreted water to surface temperature. As a result, the deposit surface temperature rises. When the surface temperature is near 0°C, it has been observed in the wind tunnel experiment (Lozowski et al., 1983) that the appearance of the deposit is very clear, and the unfrozen water started to run along the icing surface or was shed. In addition, under such a wet growth condition, the ice deposit can be spongy and the accretions could contain up to 30% of unfrozen liquid water (Lozowski et al., 1986). This factor, which may significantly enhance the accretion mass, is not taken into account in the present model due to the difficulties in theoretical estimation of the water incorporated into the ice lattice.

On the other hand the run down or shed unfrozen water may take some amount of heat with it. If the unfrozen water is shed to the air, it is a sink of heat in the heat balance equation. According to the two-stage growth hypothesis, laboratory experiment (Prodi et al., 1986a) indicated that, after penetration, first-stage deposits of high density reached a final

[6] Only under the standard conditions of Table 2, with different temperatures this height changes.

density lower than that reached by other grown at lower first-stage density. It may be because the latter have better protected air enclosures hindering water penetration; consequently, these droplets undergo only a minor increase in density due to the melting or penetration of the second stage. Therefore, if the two-stage growth hypothesis is applied to this case, the ice deposit density calculated here may still be valid. Even though the ice deposit surface temperature may reach 0°C and there is unfrozen water on the deposit surface, the ice density of the first stage of growth is already high.

### 4.3.3 THE ICING INTENSITY

The model results show the icing intensities decrease with time at the beginning of the icing process in the wet growth regime, because of the decrease in the heat exchange coefficient h and the freezing fraction. The Nusselt number $N_u$ ($= hD/k_a$) and the Reynolds number $R_e$ ($= vD\rho/\mu$) in a flow around a smooth cylinder are related at the stagnation point by Schlichting (1979):

$$N_u = R_e^{\frac{1}{2}} \tag{4.1}$$

Using this result the local heat exchange coefficient h can be expressed as:

$$h = k_a (v\rho_a/D\mu)^{\frac{1}{2}} \tag{4.2}$$

where $k_a$ is molecular thermal conductivity. Eq.(4.2) shows that at the beginning of the icing process the ice deposit diameter has a drastic increase, so that the heat exchange coefficient h decreases correspondingly.

### 4.3.4 THE SENSITIVITY OF ICE LOAD TO ATMOSPHERIC PARAMETERS

The model result shows that M is sensitive to $t_a$ in the wet growth regime, but not in the dry growth regime (upper part of Fig.3.10). This can be explained qualitatively as follows. In wet growth the icing intensity I is related to the heat flux from the icing surface and this heat flux increases with decreasing $t_a$. On the other hand, in dry growth, $t_a$ has no effect on I.

In the model results, the sensitivity of the ice load to various atmospheric parameters is shown. The sensitivity of M to the droplet diameter in Fig.3.11 is high. Whether the growth is dry (heigher than 7m) or wet (lower than 7m), M is sensitive to d. In practice, the droplet size is difficult to measure. Therefore, we are unable to predict the mass load by means of the droplet size even though M is sensitive to the droplet diameter.

The model results in Fig.3.12 shows the ice load growth for three different wind speeds, after 20 and 40 hours, respectively. It is seen that the ice load growth in either dry and wet growth condition is sensitive to the wind speed. This may be explained that at low air temperature the icing intensity changes linearly with wind speed (Lozowski, personal communication, 1987), whereas the ice load is proportional to the icing intensity (Eq.(2) in Appendix).

### 4.3.5 THE ASSUMPTIONS IN THIS MODEL

Finstad (1986) has point out that the collision efficiency work of Langmuir and Blodgett (1946) assumed that the air is in potential flow about the collecting cylinder, that only a steady-state drag force is exerted on the water droplets by the flow, and that the flow itself remains unaffected by the presence of the droplets. Also, use of Langmuir and Blodgett's steady-state viscous drag coefficient ignores buoyancy and gravitational forces. The assumptions are probably reasonable for the small liquid water content typical of cloud ($<5 g/m^3$ Finstad 1986). In the case of heavy spray with large gravitational drift over the sea surface like the condition presented here, however, the assumption is debatable. Preliminary numerical calculations by Szilder (personal communication, 1986) indicate that there is

nevertheless a very small effect of gravitational drift on the collision efficiency. This is a question which should be investigated further. In the example presented here, we assume the results are valid, because the droplets in the spray are quite large and hence have collision efficiencies near one.

The assumption in this model that the spray droplets are in thermal equilibrium with the air may also be false. Since the drops flying in the air begin with the temperature of the ocean surface, the final temperature at impact is one of the complicating factors which has so far been ignored. Stallabrass (1980) has developed a heat transfer model for the spray droplets which gives the final temperature at impact in terms of the flight time or trajectory length. However, Lozowski et al. (1986) have pointed out that because a rather arbitrary assumption about the trajectory length is made in the model, the usefulness of the model is limited.

In the model we have assumed that the droplet sizes are the same for each height. However, the relationship among droplet diameter, the liquid water content and wind speed for marine icing condition is poorly known quantitatively. Qualitative observation made in mountain fogs (Diem, 1956) and in stratiform clouds (Makkonen, 1984) have indicated that d increases with increasing w. Also, the liquid water content may decrease when the wind speed increases. In the model test, we ignored any possible droplet size change with height because of the drastic decrease in liquid water content. This could, however, result in an overestimate of ice load for the upper part of the cylindrical structure.

It is assumed in all of the previous models of cylinder icing that the wind direction is perpendicular to the icing cylinder, so that the angle $\theta$ between the wind vector and the icing cylinder axis is $90^{\circ}$. An attempt has been made in this model to take into account the effect of the angle $\theta$. The change of the angle $\theta$ is equivalent to that of the liquid water content or the drop size, which keeping $\theta = 90^{\circ}$.

Other probable sources of error in the numerical model results arise mainly from the possible irregularity of the ice deposit surface. Small deviations of the accretions from circular form is unlikely to cause large errors because the collision efficiency (McComber and Touzot,

1981), and heat transfer (Smith et al., 1983) are not very sensitive to this. However, variations in the roughness of the ice deposit surface may cause large errors, particularly in the wet growth. This factor influences the heat transfer coefficient h considerably. Increasing surface roughness moves the transition point from laminar to turbulent flow upstream, leading to increased heat transfer. Experiments have been made to examine the heat transfer from rough surfaces (Achenbach 1977, Smith et al., 1983), but it is not known how to characterize the roughness of the true accretion surface under different conditions. Lozowski et al. (1979) attempted to account for the effect of roughness on the heat transfer coefficient h in their icing model by applying Achenbach's data for the roughest cylinder tested. Based upon this study, it is strongly suggested that more experimental and theoretical work is needed to reveal the effect of the surface roughness characteristics on the heat transfer from the cylinder surface, and to determine the relationship between the degree of surface roughness and the ice growth conditions.

The author would have taken into account the effect of salinity, if the time had been available. In fact, in the wet growth process as simulated in this model, the surface temperature should be the equilibrium freezing temperature of water of the appropriate salinity. As the ice forms, salt is rejected and the salinity of the surface layer increases above that of the spray (Lozowski et al., 1986). Stallabrass (1980) used the data of Tabata (1968) in his model to establish a relationship among the surface temperature, freezing fraction and the freezing temperature of the spray, and incorporated these factors into the heat balance equation. However, both the Finnish experiments (Launiainen et al., 1983) and more recent experiments at the University of Alberta (Lozowski and Nowak, 1985) have shown that the effect of salinity on the growth rate is not a very large one. Thus, the model results may not be significantly affected by the salinity.

### 4.3.6 APPLICATION OF THE ICING MODEL

Prediction of ice accretion on real marine structures can be made by using the numerical model presented here. Since many of the structures of a ship or drilling vessel are

either cylindrical in shape or can be approximated as such, it is possible to consider every part of the marine structure to be an arbitrarily oriented cylinder. One can then use the model for each of them, and sum the resulting ice load over all of the cylinders. Of course, it is difficult to take into account the result of interactions among the various elements (Lozowski et al., 1986), such as shadowing, transport of shed, or surface water, even the heat exchage among them (if any). Nevertheless, if the dimensions of the structures are not very large compared with the distances between them, perhaps these factors can be ignored.

There are various important physical and environmental parameters which need to be considered in an icing model. From the previous discussion, we have seen that ice mass accretion is very sensitive to the air temperature and wind speed. Similarly, Lozowski and Gates (1986) have shown the influence of the major variables on the icing rate, and made comparisons among four models. They pointed out that among the six important environmental parameters, it is fairly clear that the two most important factors are the air temperature and the wind speed. Fortunately, these two factors are routinely measured meteorological parameters, which brings us more convenience in determining ice growth rate.

## Chapter 5

## CONCLUSIONS

The investigation on cylindrical ice deposit for the relative contributions of the individual component to the total heat exchange was made. The understanding of the dominant transfer ratios can be so significant that it is possible to simulate the heat exchange ratios in laboratory experiments, thereby leading to the understanding the physics of the ice accretion. In addition, these factors represent a set of new variables with which the structure of ice deposits might be correlated more satisfactorily than with icing parameters, such as air temperature, droplet temperature, liquid water content and the droplet size.

The contours of the collection efficiency and the icing intensity are plotted to demonstrate the sensitivities of these parameters to different atmospheric conditions. The change of the collection efficiency with droplet diameter or the cylinder diameter can be very complicated. It is not a linear function of either of the parameters. Moreover, the change of icing intensity can be very difficult to predict if the wind speed and air temperature change at the same time. These plots can give us a general idea of the E and I values, and they can be also used to visualize E and I without having to do the calculation.

The application of the single cylinder icing model on a marine structure shows features of the ice accretion process, and the time-evolution at different height above the sea surface. Some results obtained by the model have not been revealed by previous theoretical descriptions of icing. For example in Fig.3.9 the result shows that the freezing fraction in the wet growth can decrease at the beginning of icing, then increase again after some time. Even at 8m height, the ice growth regime changes from dry to wet growth and then changes back again under the same atmospheric condition.

The improvements of this model make it possible to describe the icing on marine structure at different heights above sea surface. The model enables us not only to estimate the total ice load on the marine structure, but also the details of icing processes with height. Taking into account the angle of wind direction enables us to consider mass load M as a function of $\theta$ angle, and relates the function $M(\theta)$ to the growth conditions. Also, we are

able to treat the function $M(\theta)$ differently in dry and wet growth regime. By using this model, the real marine structure icing prediction can be accomplished. It is the author's opinion that further studies on the following aspects would be urgently needed:

1) Further investigation on the liquid water content profile over sea surface.

2) Improvements in simulating the heat transfer coefficient for rough surfaces and study of the influence of the gravitational draft over sea surface.

3) The density parameter (Macklin, 1962) may be further justified by introducing the second stage of ice accretion.

**Bibliography**


Achenbach, E. 1977: The effect of surface roughness on the heat transfer from a circular cylinder to the cross flow of air. *International Journal of Heat and Mass Transfer*, 20, 359-369.

Bain, M. and J.F. Gayet, 1982: Contribution to the modeling of the ice accretion process: ice density variation with the impact surface angle. *Ann. Glaciol.*, 4, 19-23.

Beard,K.V. and H.R. Pruppacher, 1969: A determination of the terminal velocity and drag of small water drops by means of a wind tunnel. *J. Atmos. Sci.*, 26, 1066-1072.

Bendel, W.B., and D. Paton, 1981: A review on the effect of ice storms on the power industry. *J. Appl. Metoro.*, 20, 1445-1449.

Borisenkov, Ye. P., and I. G. Pchelko, 1975: Indicators for forecasting ship icing. USACRREL Draft Translation. No. 481.

Brown, R.D. and P. Roebber, 1985: The ice accretion problem in Canadian waters related to offshore energy and transportation. Canadian Climate Center Report 85-13, 295pp, unpublished manuscript.

Cansdale, J. T., and I. I. McNaughtan, 1977: Calculation of surface temperature and ice accretion rate in a mixed water droplet/ice crystal cloud. Tech. Rep. 77090, *Royal Aircraft Establishment*, Farnborough, U. K., 29 pp.

Comiskey, A. l., L. D. Leslie, and J. L. Wise, 1984: Superstructure icing and forecasting in Alaskan waters. Unpublished draft report submitted by the Arctic Environmental Information and Data Centre to Pacific Marine Enviromental Laboratory (NOAA), Seattle , 39 pp.

Diem, M. 1956: Ice loads on high voltage conductors in the mountains. *Archiv fur Meteorologie, Geophysik und Bioklimatologie,* Ser. B., 7, 84-85.

Dranevic, E. p., 1971: Glaze and rime Gidrometeorologitsheskoe Izdatelstvo, Leningrad, 227 pp. (in Russian).

Bendel, W. B., and D. Paton, 1981: A review on the effect of ice storms on the power industry. *J. Appl. Meteor.*, 20, 1445-1449.

Egelhofer, K. Z., Ackley, S. F. and Lynch, D. R. 1984: Computer modelling of atmospheric ice accretion and aerodynamic ice loading of transmission lines. Proceedings, Second International Workshop on Atmospheric Icing of Structures, Trondheim, (In press).

Finstad, K. J. 1986: Numerical and experimental studies of rime ice accretion on cylinders and airfoils. Ph.D. Thesis. Meteorology Division, University of Alberta.

Gent, R. W. and Cansdale, J. T. 1985: The development of mathematical modelling techniques for helicopter rotor icing. AIAA publication 85-0336, 10 pp.

Herman, G. F. 1980: Thermal radiation in arctic stratus clouds. *Quart. Jour. Roy. Meteor. Soc.*, 106, 771-780.

Horjen, I., 1981: Ice accretion on ships and marine structures. Marines structures and ships in

ice (MSSI) Report 80-01, 156pp.

Horjen, I., 1983a: Mobile platform stability. Norwegian Hydrodynamic Laboratories Report NHL 283021.

Howe, J. B., 1982: Measurements and analysis of icing and wind loads on wires. Final rep., U.S. Army Cold Regions Res. Eng. Lab., Hanover, NH, 8 pp.

Itagaki, K., 1984: Icing rate on stationary structures under marine conditions. *CRREL Report*, 84-12, 9 pp.

Jessup, R. G., 1985: Forecast techniques for ice accretion on different types of marine structures, including ships, platforms and coastal facilities. Draft report presented to WMO Commission for marine Meteorology, Oct. 1984, 90 pp.

Kachurin, L.G., L.I. Gashin, and I.A. Smirnov, 1974: Icing rate of small displacement fishing boats under various hydrometeorological conditions. Meteorologiya i Gidrologiya, 3, 50-60 (in Russian). Also available in English translation in Meteorology and Hydrology, 3, 58-71.

Langmuir, I., and K. M. Blodgett, 1946: Mathematical investigation of water droplet trajectories. G. E. Report RL--255. Reprinted in Collected Works of I. Langmuir, Pergamon Press, Vol. 10, 335-393.

Launiainen, J., M. Lyyra and L. Makkonen, 1983: A wind tunnel study of icing on marine structures. 7th International Conference on Part and Ocean Engineering under Arctic Conditions, Helsinki, Finland.

List, R. 1960: Zur Thermodynamik teilweise waesseriger Hagelkoerner. Z. angew. Math. Phys., 11, 273-306.

Lozowski, E. P. and E. M. Gates, 1986: Marine Icing Models: How do they work and how good are they? Proceedings International Workshop on Offshore Winds and Icing, Halifax, T.A. Agnew and V.R. Swail, editors, pp.102 - 122.

Lozowski, E. P., J. R. Stallabrass, and P. E. Hearty, 1983: The icing of an unheated, nonrotating cylinder. Part I: a simulation model. *J. Climate and App. Meteor.*, 22, 2053-2062.

Lozowski, E. P., J. R. Stallabrass, and P. E. Hearty, 1983: The icing of an unheated, nonrotating cylinder. Part II: Icing Wind Tunnel Experiments. *J. Climate and App. Meteor.*, 22, 2063-2074.

Lozowski, E. P., J. R. Stallabrass, and P. E. Hearty, 1979: The icing of an unheated non-rotating cylinder in liquid water droplet-ice crystal clouds. National Reserch Council of Canada Report LTR-LT-96, 61pp. [Available from NRCC, Ottawa, Canada, K1A 0R6.]

Lozowski, E. P. and A. Nowak, 1985: The design and construction of an outdoor marine icing facility. Final Technical Report under Contract KM-147-4-1255, presented to Atmospheric Environment Service of Canada, 36pp.

Lozowski, E. P., E. M. Gates, and L. Makkonen, 1986: Estimation of the icing hazard for mobile offshore drilling units. Proceedings 5th International Symposium on Offshore Mechanics and Arctic Engineering, Tokyo.

Launiainen, J., M. Lyyra, and L. Makkonen, 1983: A wind tunnel study of icing on marine structures. Paper presented at the 7th International Conference on Port and Ocean Engineering Under Arctic Conditions, Helsinki, 12pp..

Ludlam, F. H., 1958: The hail problem. Nubila, 1, 12--96.

MacArthur, C. D., Keller, J. L. and Luers, J. K. 1982: Mathematical modelling of ice accretion on airfoils. *AIAA Publication* No. 82-0284.

Macklin, W.C. 1962: The density and structure of ice formed by accretion. *Quart. Jour. Roy. Meteor. Soc.*, 88, 30-50.

Macklin, W. C. and G. S. Payne, 1967: A theoretical investigation of the ice accretion process. *Quart. Jour. Roy. Meteor. Soc.*, 93, 195--214.

McComber, P. and G. Zouzot, 1981: Calculation of the impingment of cloud droplets on a cylinder by the finite--element method. *J. Atmos. Sci.*, 38, 1027--1036.

Makkonen, L. 1984: Modelling of ice accretion on wires. *J. Climate and App. Meteor.*, Vol. 23, No.6.

Makkonen, L. 1984: Atmospheric icing on sea structures. U.S. Army CRREL Monograph 84-2, 102 pp.

Mertins, H. O. 1968: Icing on fishing vessels due to spray. Marine Observer, 38, 128-130.

Minsk, L.D., 1977: Ice accumulation on ocean structures. U.S. Army CRREL Report 77-17, 46pp.

*Nature* 1881: A singular case of shipwreck. 24: 106.

Nikiforov, Eu. P., 1982: Icing related problems, effect of line design and ice mapping. Special Rep. 83-17, U.S. Army Cold Regions Res. Eng. Lab., Hanover, NH, 239-245.

Oleskiw, M. M. 1982: A computer simulation of time--dependent rime icing on airfoils. Ph.D. Thesis, Meteorology Division, University of Alberta.

Preobrazhenskii, L. Yu., 1973: Estimate of the content of spray drops in the near--water layer of the atmosphere. *Fluid Mechanics--Soviet Research*, 2, 95--100.

Prodi, F., G. Santachiara and A. Franzini 1986: The density of accreted ice. *Quart. Jour. Roy. Meteor. Soc., Vol.* 112, 1057- 1080

Schlichting, H., 1979: Boundary-layer Theory. New York, McGraw-Hill.

Schuman, T. E. W., 1937: Theory of hailstone formation. *Quart. Jour. Roy. Meteor. Soc.*, 64, 3--21.

Smith, M.E., R.V. Arimilli and E.G. Keshock, 1983: Measurement of local heat transfer coefficient of four ice accretion shapes, Department of Mechanical and Aerospace Engineering, University of Tennessee, Final Technical Report, Part I.

Stallabrass, J. R., 1980: Trawler icing --- a compilation of work done at NRC. National Research Council Canada Report Mo-56 (NRC 19372), 103 pp.

Tabata, T. 1968: Research on prevention of ship icing. Defence Research Board, Ottawa, Canada, Translation T 95 J.

Zakrzewski, W. P., 1986: Icing of ships. Part I: Splashing a ship with spray. NOAA Technical Memorandum ERL PMEL-66.

**Appendix A**

## TIME DEPENDENCE IN THE MODEL

During the process of ice accretion on a structure, the dimensions of the ice deposit change. When the time dependence of D in Eq.(1.2) is taken into account for unchanged atmospheric conditions, then (Makkonen 1984):

$$I(t) = \frac{2}{\pi} E(t)\, n(t)\, v\, w \sin\theta \qquad (1)$$

the ice load $M_i$ per unit length of the cylinder at time $t_i$ is:

$$M_i = \int_0^{t_i} I(t) \frac{\pi}{2} D(t)\, dt = v\, w \sin\theta \int_0^{t_i} E(t)\, n(t)\, D(t)\, dt \qquad (2)$$

The calculation of the ice load M (kg $m^{-1}$) is made in a stepwise manner as follows:

$$M_i = M_{i-1} + I_{i-1} \frac{\pi}{2} D_{i-1} \Delta t \qquad (3)$$

and the ice deposit diameter $D_i$ is obtained from:

$$D_i = \left(\frac{4(M_i - M_{i-1})}{\pi \rho_i} + D_{i-1}^2\right)^{0.5} \qquad (4)$$

For each time step i the ice load M, the icing intensity I, the ice deposit diameter D, the collection efficiency E, the freezing fraction n and the density of the accreting ice

$\rho$ are calculated and given as output parameters.

The density of ice $\rho_i$ in Eq.(4) accreted during one time step is calculated using Macklin's (1962) density parameter:

$$R = \frac{-v_0 d}{2 t_s} \qquad (5)$$

where d is the droplet size in $\mu$m, $t_s$ is the surface temperature of the ice deposit in °C, and $v_0$ is the impact speed of the droplets (m/s) given by:

$$\begin{aligned} v_0 &= v\,(-0.174 + 1.464K_0 - 0.816K_0^2) && \text{for } K_0 \le 0.55 \\ v_0 &= v\,(0.561 + 0.592\log K_0 - 0.26(\log K_0)^2) && \text{for } K_0 > 0.55 \end{aligned} \qquad (6)$$

where $K_0$ is determined from Eq.(1.9).

The ice density $\rho$ (g cm$^{-3}$) is determined from (7) (Makkonen, 1984) which is based on Macklin (1962) and the measurements with a rotating cylinder in natural icing conditions by Bain and Gayet (1982):

$$\begin{aligned} \rho &= 0.11\,R^{0.76} && \text{for } R \le 10 \\ \rho &= R\,(R + 5.61)^{-1} && \text{for } 10 < R \le 60 \\ \rho &\doteq 0.92 && \text{for } R > 60 \end{aligned} \qquad (7)$$

**Appendix B**

## LIST OF COMPUTING PROGRAM

```
      ********************VARIABLE DICTIONARY**********************
C
C
C           PI              -CONSTANT VALUE (=3.1415926)
C           DA              -DENSITY OF THE AIR.
C           DW              -DENSITY OF WATER.
C           LF              -LATENT HEAT OF FREEZING.
C           LE              -LATENT HEAT OF EVAPORATION.
C           CP              -SPECIFIC HEAT AT CONSTANT PRESSURE.
C           KL              -A CONSTANT USED IN THE MODEDL (=0.62).
C           A               -CONSTANT VALUE.
C           EO              -VAPOR PERSSURE AT TEMPERATURE=OC.
C           CW              -SPECIFIC HEAT OF WATER.
C           PA              -PRESSURE OF THE AIR.
C           SIGMA           -STEFAN-BOLTZMAN CONSTANT.
C           CI              -SPECIFIC HEAT OF ICE.
C           LS              -LETENT HEAT OF SUBLIMATION.
C           D               -DROPLET DIAMETER.
C           TA              -AIR TEMPERATURE.
C           UA              -ABSOLUTE VISCOSITY OF AIR.
C           KA              -THERMAL CONDUCTIVITY OF AIR.
C           EA              -VAPOR PRESSURE AT TA.
C           H3              -AVERAGE WAVE HEIGHT.
C           PW              -PHASE SPEED OF THE WAVE.
C           DRC             -PARAMETER TO CONVERT DEGREES TO RADIANS.
C           (X1,Y1,Z1)      -COORDINATES OF THE ICING CYLINDER.
C           (X2,Y2,Z2)      -COORDINATES OF THE ICING CYLINDER.
C           SISITA          -SINE FUNCTION OF THE ANGLE THETA.
C           COSITA          -COSINE FUNCTION OF THE ANGLE THETA.
C           V               -WIND SPEED.
C           W               -LIQUID WATER CONTENT.
C           RED             -DROPLET REYNOLDS NUMBER.
C           RE              -CYLINDER REYNOLDS NUMBER.
C           K               -INERTIA PARAMETER.
C           E               -COLLISION EFFICIENCY.
C           EM              -COLLISION EFFICIENCY BY USING THE MVD.
C           TS              -SURFACE TEMPERATURE OF THE ICE DEPOSIT.
C           T               -TIME STEP.
C           M(J)            -UPTATED ICE LOAD.
C           RA(J)           -MASS GROTH RATE.
C           VO              -IMPACT VELOCITY.
C           DE(J)           -DENSITY OF THE ACCRETED ICE.
C           DC(J)           -UPDATED ICE DEPOSIT DIAMETER.
C           TIDD(J)         -TOTAL ICE DEPOSIT DENSITY.
C           QF(J)           -TOTAL HEAT EXCHANGE.
C           QCP(J)          -HEAT EXCHANGE DUE TO ACCRETION OF SUPERCOOLED WATER.
C           QCC(J)          -HEAT EXCHANGE DUE TO CONDUCTION/CONVECTION.
C           QES(J)          -HEAT EXCHANGE DUE TO EVAPORATION/SUBLIMATION.
C           RCC(J)          -HEAT EXCHANGE RATIO DUE TO CONDUCTION/CONVECTION.
C           RES(J)          -HEAT EXCHANGE RATIO DUE TO EVAPORATION/SUBLIMATION.
C       ******************************************************************
C
C
C
      REAL*4 I(1000),E(1000),N(1000),V,W,UA,H,KA,TA,EA,NU,
     *   PI,EM,KO,RED,K,DA,D,U,DW,DC(1000),F,F1,ES1,LS,ES,CI,
     *   LF,LE,CP,KL,A,EO,CW,PA,R,SIGMA,M(1000),DE(4000),VO,
     *   TIME(100),TIDD(1000),RA(1000),TITV,SISITA,
     *   U10,UO,H3,BO,B1,B2,B3,B4,B5,FAI,X1,X2,SITA,TS,
     *   Y1,Y2,Z1,Z2,USTAR,CO,C1,C2,C3,C4,C5,ARFA,PW,VR,VS,
```

```
     *   QF(100),QCP(100),QCC(100),QSE(100)
      DIMENSION X(10,14),YY(14,10)
      INTEGER ZZ, II, RIG,Z,KK
C
C  CONSTANT VALUES
C
          PI=3.141593
          DA=1.2923
          DW=1000.
          LF=3.34E5
          LE=2.5E6
          CP=1004.
          KL=0.69
          A=8.1E7
          EO=6.11E2
          CW=4270.
          PA=101300
          SIGMA=5.67E-8
          CI=2106.
          LS=(677.0/2.38844)*1.0E04
          D=50.E-5
          TA=-8.
          UA=1.718E-05+5.1E-08*TA
          KA=0.0243+0.000073*TA
          EA=(((.000259*TA+.027487)*TA+1.4472)*TA+44.26)*TA+609.9
             READ(5,*)U10,UO,BO,B1,B2,B3,B4,B5,FAI
             READ(5,*)CO, C1, C2, C3, C4, C5
          DRC=3.14159265/180.
          H3=BO+B1*U10+B2*U10**2+B3*U10**3+B4*U10**4+B5*U10**5
          PW=CO+C1*U10+C2*U10**2+C3*U10**3+C4*U10**4+C5*U10**5
          VR=1.559*PW
C
C  CALCULATION OF THE SINE FUNCTION OF THE ANGLE THETA
C
        READ(5,*)X1,Y1,Z1,X2,Y2,Z2
        IF(((X1-X2)**2+(Y1-Y2)**2+(Z1-Z2)**2).EQ.0.) THEN
              SISITA=10.E-9
        ELSE
              COSITA=(COS(FAI*DRC)*(Y2-Y1)+SIN(FAI*DRC)*(X2-X1))/
     $        ((X2-X1)**2+(Y2-Y1)**2+(Z2-Z1)**2)**0.5
              SISITA=(1-COSITA**2)**0.5
        END IF
          IF(SISITA.EQ.0.) SISITA=10.E-9
C
C  DO LOOP START HERE FOR DIFFERENT HEIGHT
C
             V= 15.
          DO 1600 Z=3,16
               W=6.1457E-5*H3*VR*VR*EXP(-0.55*(Z-3.))
               RED=DA*D*V/UA
               T=3600.
               DC(1)=0.01
               M(1)=0.
C
C  ANOTHER DO LOOP FOR TIME EVOLUTION
C
             DO 1200 J=1,100
                  K= (DW*V*(D*D))/(9.*UA*DC(J))
                  KO= K/(.087*RED**(0.76*RED**(-0.027))+1.)
C
```

```
C  CALCULATE THE COLLISION EFFICIENCY
C
                      IF(KO.GT.0.8) GOTO 200
                      IF(KO.GT..125)GOTO 250
                        EM=0.0
                        GOTO 300
 200                    EM=(KO**1.1)/((KO**1.1)+1.426)
                        GOTO 300
 250                    EM=0.5*(ALOG10(8*KO))**1.6
 300                    E(J)=0.69*EM**0.67+0.31*EM**1.67
C
C  CALCULATE THE ICE INTENSITY
C
                   RE=DA*DC(J)*V/UA
                   NU=0.032*RE**0.85
                   H=(KA*NU)/DC(J)
                   N(J)=((PI*H)/(2.*E(J)*V*W*SISITA*LF))*((-TA)
     $                  +((KL*LE*(EO-EA))/(CP*PA))-((0.79*V*V)/
     $                  (2*CP)))-(TA*(CW+((PI*SIGMA*A)
     $                   /(2*E(J)*V*W*SISITA))))/LF
                   IF(N(J).GT.1) N(J)=1
                   I(J)=(2./PI)*E(J)*N(J)*V*W*SISITA
C
C  CALCULATE THE SURFACE TEMPERATURE
C
              TS=0
 650          ES=(((.000259*TS+.027487)*TS+1.4472)*TS+44.26)
     $             *TS+609.92
              F=(2./PI)*E(J)*V*W*SISITA*(LF+CW*TA-CI*TS)-H*((TS-TA)
     $            +((0.62*LS)/(CP*PA))*(ES-EA)-((0.79*V*V)/(2*CP)
     $            ))-(SIGMA*A)*(TS-TA)
              ES1=4.*.000259*TS**3+3*.027487*TS**2+2*1.4472*TS+44.2
              F1=(2./PI)*E(J)*V*W*SISITA*CI*(-1)-H-((H*0.62*LS)/
     $            (CP*PA))*ES1-(SIGMA*A)
              TS1NEW=(-1)*(F/F1)+TS
C
                   IF(ABS(TS1NEW-TS).LT..01) THEN
                       TS=TS1NEW
                   ELSE
                       TS=TS1NEW
                       GOTO 650
C
                    IF(TS.GE.0) TS=-1.E-6
C
C  CALCULATE ICE LOAD: M(J+1)
C
             M(J+1)=M(J)+I(J)*(PI/2.)*DC(J)*T
C
C  CALCULATE MASS GROWTH RATE
C
             RA(J)=(M(J+1)-M(J))
C
C  CALCULATE IMPACT VELOCITY VO
C
           IF(KO.LE.0.55) VO=V*(-0.174+1.464*KO-0.816*KO*KO)
           IF(KO.GT.0.55) VO=V*(0.561+0.592*(ALOG10(KO))-0.26*
     $                        (ALOG10(KO))*ALOG10(KO))
C
C  CALCULATE DENSITY OF ACCRETING ICE : DE(J+1)
C
```

```
          R=-(VO*D*1000000)/(2*TS)
              IF(R.LT.0.9) DE(J+1)=0.1
              IF((R.GE.0.9).AND.(R.LE.10.)) DE(J+1)=0.11*(R**0.76)
              IF((R.GT.10.).AND.(R.LE.60.)) DE(J+1)=R*(1/(R+5.61))
              IF(R.GT.60.) DE(J+1)=0.92
C
                   DE(J+1)=DE(J+1)*1000.
C
C   CALCULATE ICE DEPOSIT DIAMETER: DC(J+1)
C
      DC(J+1)=SQRT((4.*(M(J+1)-M(J))/(PI*DE(J+1)))+DC(J)*DC(J))
C
C   CALCULATE THE TOTAL ICE DEPOSIT DENSITY: TIDD
C
      TIDD(J+1)=4.*M(J+1)/(PI*(DC(J+1)*DC(J+1)-DC(1)*DC(1)))
      TITV=T/60
C
C   CALCULATE THE HEAT EXCHANGE RATIOS
C
              QF(J)=(2/PI)*E(J)*V*W*N(J)*LF
              QCP(J)=(2/PI)*E(J)*V*W*N(J)*(CW*TA-CI*TS)
              QCC(J)=H*(TS-TA)
              QSE(J)=(H*0.69*LS*(ES-EA))/(CP*PA)
1200     CONTINUE
C
C  PRINT OUT THE RESULT
C
      WRITE(6,6668)RA(10),RA(20),RA(40),RA(60),RA(80),RA(100)
6668  FORMAT(2X,6F9.4)
C
C  RA(J) CAN BE CHANGED INTO ANY OTHER PARAMETER SUCH AS
C
C      WRITE(6,6669)QCC(2),QCC(4),QCC(6),QCC(8),QCC(10),QCC(20),
C     #             QCC(40),QCC(60),QCC(80),QCC(100)
C6669  FORMAT(2X,10(F10.2))
C
C   WHEN YOU NEED THE PRINTED RESULT TO BE FUNCTION OF TIME
C       SUE THE FOLLOWING DO LOOP
C
C            DO 7001 IIN=1,5
C                X(IIN+5,Z+1)=N(IIN*20)
C7001        CONTINUE
C
1600 CONTINUE
C            DO 7002 IIN=1,10
C            WRITE(6,7005) (X(IIN,J),J=1,14)
C7002        CONTINUE
C7005        FORMAT (1X,14(F8.3,2X))
C
C
C ALL THE DO LOOPS END UP HERE
C
C
     STOP
     END
```